[6] J.R. Wall, M. Salvi, N. Bernard, A. Boucher, D. Haegert, Thyroid-associated ophthalmopathy-A model for the association of organ-specific autoimmune disorder, Immunol. Today 12 (1991) 150–153.
[7] H.B. Burch, L. Wartofsky, Graves' ophthalmopathy: current concepts regarding pathogenesis and management, Endocrinol. Rev. 14 (1993) 747–793.
[8] F. Karlsson, P. Dåhlberg, P. Jansson, K. Westermark, P. Enoksson, Importance of TSH receptor activation in the development of severe endocrine ophthalmopathy, Acta Endocrinol. 121 (1989) 132–141.
[9] R.S. Bahn, C.M. Dutton, N. Natt, W. Joba, C. Spitzweg, E.A. Heufelder, Thyrotropin receptor expression in Graves' orbital adipose/connective tissues: potential autoantigen in Graves' ophthalmopathy, J. Clin. Endocrinol. Metab. 83 (1998) 998–1002.
[10] R. Paschke, A. Metcalfe, L. Alcalde, G. Vassart, A. Weetman, M. Ludgate, Presence of nonfunctional thyrotropin receptor variant transcripts in retroocular and other tissues, J. Clin. Endocrinol. Metab. 79 (1994) 1234–1238.
[11] R.S. Bahn, Pathophysiology of Graves' ophthalmopathy: the cycle of disease, J. Clin. Endocrinol. Metab. 88 (2003) 1939–1946.
[12] M. Salvi, A. Miller, J.R. Wall, Human orbital tissue and thyroid membranes express a 64kDa protein which is recognized by autoantibodies in the serum of patients with thyroid-associate ophthalmopathy, FEBS Lett. 232 (1988) 135–139.
[13] Y. Hiromatsu, M. Sato, K. Tanaka, S. Shoji, K. Nonaka, M. Chinami, H. Fukazawa, Significance of anti-eye muscle antibody in patients with thyroid-associated ophthalmopathy by quantitative Western blot, Autoimmunity 14 (1991) 1–8.
[14] Y-J. Wu, S.E.M. Clarke, P. Shepherd, Prevalence and significance of antibodies reactive with eye muscle membrane antigens in sera from patients with Graves' ophthalmopathy and other thyroid and nonthyroid disorders, Thyroid 8 (1998) 167–174.
[15] S. Kubota, K. Gunji, C. Stolarski, J.S. Kennerdell, J.R. Wall, Reevaluation of the prevalences of serum autoantibodies reactive with eye muscle antigens in patients with thyroid autoimmunity and ophthalmopathy, Thyroid 8 (1998) 175–179.
[16] S. Kubota, K. Gunji, B.A.C. Ackrell, B. Cochran, C. Stolarski, S. Wengrowicz, J.S. Kennerdell, Y. Hiromatsu, J. Wall, The 64-kDa eye muscle protein is the flavoprotein subunit of mitochondrial succinate dehydrogenase: the corresponding serum antibodies are good markers of an immune-medicated damage to the eye muscle in patients with Graves' hyperthyroidism, J. Clin. Endocrinol. Metab. 83 (1998) 433–447.
[17] K. Gunji, A. De Bellis, S. Kubota, J. Swanson, S. Wengrowicz, B. Cochran, B.A. Ackrell, M. Salvi, A. Bellastella, A. Bizzarro, A.A. Sinisi, J.R. Wall, Serum antibodies reactive against the flavoprotein subunit of succinate dehydrogenase are sensitive and specific markers of eye muscle autoimmunity in patients with Graves' hyperthyroidism, J. Clin. Endocrinol. Metab. 84 (1999) 16–22.
[18] Q. Dong, M. Ludgate, G. Vassart, Cloning and sequencing of a novel 64-kDa autoantigen recognized by patients with autoimmune thyroid disease, J. Clin. Endocrinol. Metab. 72 (1991) 1375–1381.
[19] A. Barsouk, S. Wengrowicz, D. Scalise, C. Stolarski, V. Nebes, M. Sato, J.R. Wall, New assays for the measurement of serum antibodies reactive with eye muscle membrane antigens confirm their significance in thyroid-associated ophthalmopathy, Thyroid 5 (1995) 195–200.
[20] T.C. Chang, T.J. Chang, Y.S. Huang, K.M. Hua, R.J. Su, S.C.S. Kao, Identification of autoantigen recognized by autoimmune ophthalmopathy sera with immunoblotting correlated with orbital computed tomography, Clin. Immunol. Immunopathol. 65 (1992) 161–166.
[21] M. Salvi, N. Bernard, A. Miller, Z.G. Zhang, E. Gardini, J.R. Wal, Prevalence of antibodies reactive with a 64kDa eye muscle membrane antigen in thyroid-associated ophthalmopathy, Thyroid 1 (1991) 207–213.
[22] K. Gunji, A. De Bellis, A.W. Li, M. Yamada, S. Kubota, B. Ackrell, S. Wengrowicz, A. Bellastella, A. Bizzarro, A. Sinisi, J.R. Wall, Cloning and characterization of the novel thyroid and eye muscle shared protein G2s: autoantibodies against G2s are closely associated with ophthalmopathy in patients with Graves' hyperthyroidism, J. Clin. Endocrinol. Metab. 85 (2000) 1641–1647.
[23] M. Yamada, A.W. Li, K.A. West, C.H. Chang, J.R. Wall, Experimental model for ophthalmopathy in BALB/c and outbred (CD-1) mice genetically immunized with G2s and the thyrotropin receptor, Autoimmunity 35 (2002) 403–413.
[24] A. De Bellis, A. Bizzarro, M. Conte, C. Coronella, S. Solimeno, S. Perrino, D. Sansone, M. Guaglione, J.R. Wall, A. Bellastella, Relationship between longitudinal behavior of some markers of eye autoimmunity and changes in ocular findings in patients with Graves' ophthalmopathy receiving corticosteroid therapy, Clin. Endocrinol. (Oxf.). 59 (2003) 388–395.
[25] K.C. Ossoinig, The role of standardized echography in Graves' disease, Acta Ophthalmol. (Copenh) 204 (1992) 81.
[26] X.P. Pang, J.M. Hershman, M. Chung, A.E. Pekary, Characterization of tumor necrosis factor-α receptors in human and rat thyroid cells and regulation of the receptors by thyrotropin, Endocrinology 125 (1989) 1783–1788.
[27] T. Ito, T. Seyama, T. Hayashi, K. Dohi, T. Mizuno, K. Iwamoto, N. Tsuyama, N. Nakamura, M. Akiyama, Establishment of two human thyroid carcinoma cell lines (8305C, 8505C) bearing p53 gene mutations, Int. J. Oncol. 4 (1994) 583–586.
[28] M. Derwahl, M. Kuemmel, P. Goretzki, H. Schatz, M. Broecker, Expression of the human TSH receptor in a human thyroid carcinoma cell line that lacks an endogenous TSH receptor, Biochem. Biophys. Res. Commun. 191 (1993) 1131–1138.
[29] J.A. Fagin, K. Matsuo, A. Karmakar, D.L. Chen, S.H. Tang, H.P. Koeffler, High prevalence of mutations of the p53 gene in poorly differentiated human thyroid carcinomas, J. Clin. Invest. 91 (1993) 179–184.
[30] T.P. Solovyeva, Endocrine ophthalmopathies. Problems of rational classification, Orbit 3 (1989) 193–198.
[31] S.E. Lux, K.M. John, V. Bennett, Analysis of cDNA for human erythrocyte ankyrin indicates a repeated structure with homology to tissue-differentiation and cell-cycle control proteins, Nature 344 (1990) 36–42.

Comparison of Frequency of Interferon-γ–Positive CD4+ T Cells Before and After Percutaneous Coronary Intervention and the Effect of Statin Therapy in Patients With Stable Angina Pectoris

Tomoko Tanaka, MD, Hirofumi Soejima, MD, PhD, Nobutaka Hirai, MD, PhD, Tomohiro Sakamoto, MD, PhD, Michihiro Yoshimura, MD, PhD, Ichiro Kajiwara, MD, Yuji Miyao, MD, PhD, Kazuteru Fujimoto, MD, PhD, Hiroo Miyagi, MD, PhD, Atsushi Irie, PhD, Yasuharu Nishimura, MD, PhD, and Hisao Ogawa, MD, PhD

We investigated the effect of statin therapy on T-cell activation in patients who underwent percutaneous coronary intervention by using flow cytometric analysis. The increased frequency of interferon-γ–positive CD4+ T cells after percutaneous coronary intervention was significant in the group treated without statins but not in the group treated with statins. ©2004 by Excerpta Medica, Inc.

(Am J Cardiol 2004;93:1547–1549)

Atherosclerosis has been demonstrated to be an inflammatory process involving various immune cells,[1] in particular T cells and macrophages in plaque.[2] Another study using flow cytometry has shown that activated T cells are related to plaque instability. Liuzzo et al[3] measured the frequency of activated T cells treated with phorbol myristate acetate and ionomycin. We recently reported a significant increase in activated T cells in patients with unstable angina.[4] In addition, percutaneous coronary intervention (PCI) has been shown to induce an inflammatory response locally[5] and systemically,[6] and hydroxymethyl-glutaryl-coenzyme A reductase inhibitors (statins) have been found to affect inflammation.[7] In other research, clinical trials have shown that statins decrease the incidence of early death and recurrent ischemia in patients undergoing PCI.[8] Therefore, we investigated the effect of statin therapy on T-cell activation in patients who underwent PCI using flow cytometric analysis.

• • •

The study population consisted of 41 consecutive patients (24 men and 17 women; mean age 72 ± 7 years) with stable angina pectoris who underwent elective single-vessel PCI between July 2002 and June 2003. Exclusion criteria were inflammatory disease, collagen disease, infection, unstable angina, acute myocardial infarction, and heart failure. The patients were assigned to 1 of 2 groups depending on whether statins were administered before admission: statin-treated group or non–statin-treated group. Informed consent was obtained from each patient.

PCI was performed according to a standard technique in 1 vessel per patient. All patients received an intravenous injection of 5,000 IU of heparin and intracoronary injection of isosorbide dinitrate during angioplasty, in which a balloon was positioned at the stenotic region and inflated. Adjunctive stent implantation was performed if the residual diameter stenosis

TABLE 1 Clinical Characteristics of Statin-Treated Group and Non–Statin-Treated Group

Variable	Statin Treatment + (n = 17)	Statin Treatment 0 (n = 24)
Age (yrs)	69 ± 8	73 ± 7
Men	9 (53%)	15 (63%)
Body mass index (kg/cm²)	24.2 ± 2.3	23.1 ± 3.2
Total cholesterol (mg/dl)	205 ± 53	201 ± 43
Triglyceride (mg/dl)	144 ± 57	120 ± 46
HDL cholesterol (mg/dl)	47 ± 8	49 ± 17
LDL cholesterol (mg/dl)	135 ± 50	126 ± 28
Diabetes mellitus	6 (35%)	7 (29%)
Systemic hypertension	14 (82%)	21 (88%)
Smoker	4 (24%)	5 (21%)
No. of coronary arteries narrowed ≥75% in diameter		
1	6 (35%)	10 (42%)
2	10 (59%)	10 (42%)
3	1 (6%)	4 (17%)
Stent implantation	12 (71%)	20 (83%)
Medications		
Aspirin	15 (88%)	22 (92%)
ACE inhibitors	3 (18%)	5 (21%)
Calcium antagonist	12 (71%)	16 (67%)
β Blockers	3 (18%)	5 (21%)
Nitrates	4 (24%)	6 (25%)

Data are presented as mean ± SD or number of patients (percents).
ACE = angiotensin-converting enzyme; HDL = high density lipoprotein; LDL = low density lipoprotein.

From the Departments of Cardiovascular Medicine and Immunogenetics, Graduate School of Medical Sciences, Kumamoto University, Kumamoto; and the Department of Cardiovascular Center, Kumamoto National Hospital, Kumamoto, Japan. This study was supported in part by Japan Heart Foundation Research grants for cardiovascular disease (14C-1 and 14C-4) from the Ministry of Labor, and Health Welfare, Tokyo, Japan; a Grant-in-Aid for Scientific Research (B15390248), and a Grant-in-Aid for Young Scientists (B14770319) from the Ministry of Education, Culture, Sports, Science, and Technology, Tokyo, Japan; and a Smoking Research Foundation Grant for Biomedical Research Foundation, Tokyo, Japan. Dr. Soejima's address is: Department of Cardiovascular Medicine, Graduate School of Medical Sciences, Kumamoto University, 1-1-1 Honjo, Kumamoto City 860-8556, Japan. E-mail: yuuki@gpo.kumamoto-u.ac.jp. Manuscript received November 7, 2003; revised manuscript received and accepted February 24, 2004.

0002-9149/04/$–see front matter
doi:10.1016/j.amjcard.2004.02.070

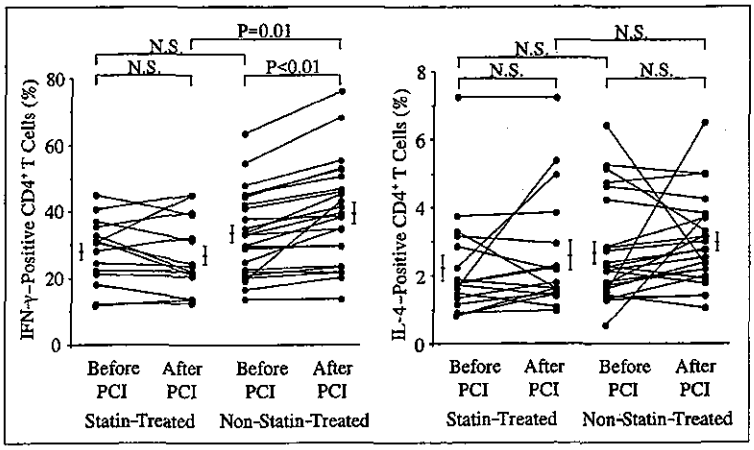

FIGURE 1. Frequency of IFN-γ–positive *(left)* and interleukin-4 (IL-4)–positive *(right)* $CD4^+$ T cells before and after PCI (mean ± SE).

was ≥30% and there was a complex coronary dissection. All PCI procedures were successful.

Peripheral blood samples were obtained with a 21-gauge needle through clean vein puncture from all patients on admission for the measurement of lipid levels. Whole blood samples were also taken before PCI and 2 days after PCI for measurement of interferon-γ (IFN-γ)–positive $CD4^+$ T-cell frequencies. For each sample, 3 ml of blood was drawn into a heparinized Vacutainer.

Whole blood was incubated at 37°C and in 5% carbon dioxide for 4 hours in nonactivating medium (RPMI 1640 supplemented with 10% fetal calf serum and 40 μg/ml of brefeldin A; Sigma Chemical Co., St. Louis, Missouri) or activating medium (nonactivating medium with 40 ng/ml of phorbol myristate acetate [Calbiochem, San Diego, California] and 4 μg/ml of ionomycin [Sigma Chemical Co.]). After being washed with ice-cold phosphate buffered saline, cells were recovered by centrifugation and adjusted to 5×10^5 white blood cells per test. Cell surfaces were stained with anti-CD4-Cy-Chrome monoclonal antibody (BD Pharmingen, San Jose, California), and fixation and permeabilization were performed with IntraPrep reagent (Beckman Coulter, Hialeah, Florida). Intracellular cytokines were stained with anti–IFN-γ fluorescein isothiocyanate monoclonal antibody and anti–interleukin-4 phycoerythrin monoclonal antibody (Beckman Coulter). IFN-γ–positive $CD4^+$ T cells and interleukin-4–positive $CD4^+$ T cells were analyzed using 3-color flow cytometry with the FACScan cytometer and CellQuest software (Becton Dickinson). Nonspecific staining with the isotype-matched control monoclonal antibody was <1%.

Continuous values were expressed as mean ± SD and were compared with unpaired *t* test. Categorical data were expressed as frequencies and percentages. Chi-square test was used for the analysis of categorical data. Changes in frequencies of IFN-γ–positive $CD4^+$ T cells before and after PCI were compared with the Wilcoxon signed-ranks test. Differences in these frequencies between the statin-treated and non–statin-treated groups were compared with the Mann-Whitney U test. A p value <0.05 was considered statistically significant.

Twenty-four of the 41 patients were assigned to the non–statin-treated group and the remaining 17 were assigned to the statin-treated group. Nine patients were treated with pravastatin, 4 patients with atorvastatin, and 4 patients with simvastatin. Clinical characteristics of the statin-treated group and the non–statin-treated group are listed in Table 1. There was no significant difference between the 2 groups with respect to characteristics and medications.

After PCI, the frequency of IFN-γ–positive $CD4^+$ T cells increased significantly from 33.64 ± 12.66% to 39.63 ± 15.42% in the non–statin-treated group (p <0.01). The frequency increased in 22 of 24 patients in the non–statin-treated group. In contrast, frequency after PCI did not significantly change (from 28.10 ± 9.68% to 27.06 ± 11.32%) in the statin-treated group. The frequency increased in 7 of 17 patients in the statin-treated group (Figure 1). The change in the frequency of interleukin-4–positive $CD4^+$ T cells was not significant in the statin-treated group or the non–statin-treated group.

• • •

The results of the present study showed that the frequency of IFN-γ–positive $CD4^+$ T cells significantly increased in the non–statin-treated group after PCI. The frequency after PCI increased in 22 of 24 patients in the non–statin-treated group. Conversely, the frequency did not significantly change in the statin-treated group. The frequency increased in 7 of 17 patients in the statin-treated group. The frequency decreased in the remaining 10 patients. Changes in frequency of interleukin-4–positive $CD4^+$ T cells in the statin-treated and the non–statin-treated groups between before and after PCI were not significant.

PCI induces an inflammatory response locally and systemically.[9] PCI causes plaque rupture, hemorrhage, arterial wall damage, and release of inflammatory factors with leukocyte and platelet activation.[10] A positive association between invasion of T cells and recurrence of unstable angina after PCI has also been found.[11] These findings agree with our observation of a significant increase in T-cell activation after PCI in the non–statin-treated group. Statins have been found to provide early benefits in patients undergoing PCI.[12] Experimental studies have supported the view that statins reduce inflammation[13] and that treatment with statins decreases the number of inflammatory cells in atherosclerotic plaques.[14] In an in vitro study, Kwak et al[15] observed that statin treatment inhibited T-cell proliferation and differentiation through decreased expression of major histocompatibility complex II

mRNA, and Weitz-Schmidt et al[16] reported that several statins impaired T-cell stimulation by directly binding to the lymphocyte function-associated antigen-1 regulatory site on leukocytes. Further, Youssef et al[17] recently demonstrated that statins suppressed secretion of IFN-γ from T cells in experimental autoimmune encephalomyelitis. In the present study, statins decreased T-cell activation after PCI, which correlates with published results.

1. Libby P. Inflammation in atherosclerosis. *Nature* 2002;420:868–874.
2. Hansson GK. Immune mechanisms in atherosclerosis. *Arterioscler Thromb Vasc Biol* 2001;21:1876–1890.
3. Liuzzo G, Kopecky SL, Frye RL, O'Fallon WM, Maseri A, Goronzy JJ, Weyand CM. Perturbation of the T-cell repertoire in patients with unstable angina. *Circulation* 1999;100:2135–2139.
4. Soejima H, Irie A, Miyamoto S, Kajiwara I, Kojima S, Hokamaki J, Sakamoto T, Tanaka T, Yoshimura M, Nishimura Y, Ogawa H. Preference toward a T-helper type 1 response in patients with coronary spastic angina. *Circulation* 2003;107:2196–2200.
5. Serrano CV Jr, Ramires JA, Venturinelli M, Arie S, D'Amico E, Zweier JL, Pileggi F, da Luz PL. Coronary angioplasty results in leukocyte and platelet activation with adhesion molecule expression. Evidence of inflammatory responses in coronary angioplasty. *J Am Coll Cardiol* 1997;29:1276–1283.
6. Azar RR, McKay RG, Kiernan FJ, Seecharran B, Feng YJ, Fram DB, Wu AH, Waters DD. Coronary angioplasty induces a systemic inflammatory response. *Am J Cardiol* 1997;80:1476–1478.
7. Plenge JK, Hernandez TL, Weil KM, Poirier P, Grunwald GK, Marcovina SM, Eckel RH. Simvastatin lowers C-reactive protein within 14 days: an effect independent of low-density lipoprotein cholesterol reduction. *Circulation* 2002; 106:1447–1452.
8. Serruys PW, de Feyter P, Macaya C, Kokott N, Puel J, Vrolix M, Branzi A, Bertolami MC, Jackson G, Strauss B, Meier B. Fluvastatin for prevention of cardiac events following successful first percutaneous coronary intervention: a randomized controlled trial. *JAMA* 2002;287:3215–3222.
9. Inoue T, Uchida T, Yaguchi I, Sakai Y, Takayanagi K, Morooka S. Stent-induced expression and activation of the leukocyte integrin Mac-1 is associated with neointimal thickening and restenosis. *Circulation* 2003;107:1757–1763.
10. Farb A, Sangiorgi G, Carter AJ, Walley VM, Edwards WD, Schwartz RS, Virmani R. Pathology of acute and chronic coronary stenting in humans. *Circulation* 1999;99:44–52.
11. Arbustini E, De Servi S, Bramucci E, Porcu E, Costante AM, Grasso M, Diegoli M, Fasani R, Morbini P, Angoli L, et al. Comparison of coronary lesions obtained by directional coronary atherectomy in unstable angina, stable angina, and restenosis after either atherectomy or angioplasty. *Am J Cardiol* 1995;75: 675–682.
12. Chan AW, Bhatt DL, Chew DP, Quinn MJ, Moliterno DJ, Topol EJ, Ellis SG. Early and sustained survival benefit associated with statin therapy at the time of percutaneous coronary intervention. *Circulation* 2002;105:691–696.
13. Rezaie-Majd A, Prager GW, Bucek RA, Schernthaner GH, Maca T, Kress HG, Valent P, Binder BR, Minar E, Baghestanian M. Simvastatin reduces the expression of adhesion molecules in circulating monocytes from hypercholesterolemic patients. *Arterioscler Thromb Vasc Biol* 2003;23:397–403.
14. Crisby M, Nordin-Fredriksson G, Shah PK, Yano J, Zhu J, Nilsson J. Pravastatin treatment increases collagen content and decreases lipid content, inflammation, metalloproteinases, and cell death in human carotid plaques: implications for plaque stabilization. *Circulation* 2001;103:926–933.
15. Kwak B, Mulhaupt F, Myit S, Mach F. Statins as a newly recognized type of immunomodulator. *Nat Med* 2000;6:1399–1402.
16. Weitz-Schmidt G, Welzenbach K, Brinkmann V, Kamata T, Kallen J, Bruns C, Cottens S, Takada Y, Hommel U. Statins selectively inhibit leukocyte function antigen-1 by binding to a novel regulatory integrin site. *Nat Med* 2001;7:687–692.
17. Youssef S, Stuve O, Patarroyo JC, Ruiz PJ, Radosevich JL, Hur EM, Bravo M, Mitchell DJ, Sobel RA, Steinman L, Zamvil SS. The HMG-CoA reductase inhibitor, atorvastatin, promotes a Th2 bias and reverses paralysis in central nervous system autoimmune disease. *Nature* 2002;420:78–84.

Risk Factors and Outcomes in Patients With Coronary Artery Aneurysms

Timir S. Baman, MD, Jason H. Cole, MD, Chandan M. Devireddy, MD, and Laurence S. Sperling, MD

Previous small series have provided conflicting data on the association between coronary artery aneurysms and traditional cardiac risk factors, as well as limited information on patient outcomes. This investigation sought to determine whether the presence of coronary artery aneurysms has an adverse affect on patient outcomes. The results show that coronary aneurysms were an independent predictor of mortality, and overall 5-year survival in patients with aneurysms was only 71%. We believe that clinicians should aggressively monitor and modify coronary risk factors in patients with coronary aneurysms.

(Am J Cardiol 2004;93:1549–1551)

From the University of Chicago Hospitals, Chicago, Illinois; and the Emory University School of Medicine, Atlanta, Georgia. Dr. Baman's address is: Department of Internal Medicine, University of Chicago, 5841 S Maryland Avenue, MC 7082, Chicago, Illinois 60637. E-mail: tbaman@uchospitals.edu.

Manuscript received December 16, 2003; revised manuscript received and accepted March 1, 2004.

Many questions exist regarding clinical risk factors and long-term prognosis of patients with coronary aneurysms exist. Multivariate analysis of coronary aneurysms as a correlate of long-term mortality has not been done in a large series. To better study this issue, we identified a large population with coronary aneurysms documented by strict angiographic criteria.

• • •

Information on all patients who underwent coronary angiography at Emory University Hospitals between 1995 and 2003 were included in a cardiac database. Patient variables recorded were gender, age, hypertension (defined by current or previous therapy or a history of blood pressure >140/95 mm Hg), history of coronary artery disease (CAD), smoking history, hyperlipidemia (per previous diagnosis), and history of and type of diabetes mellitus. Diabetes was defined by ongoing oral or insulin therapy or diet control, provided the clinician also had laboratory evidence of hyperglycemia. Follow-up data were obtained by telephone interview and hospital encounters.

All patients with the terms "coronary aneurysm" or "coronary ectasia" in their catheterization reports were

0002-9149/04/$–see front matter
doi:10.1016/j.amjcard.2004.03.011

INFECTION AND IMMUNITY, June 2004, p. 3592–3603 Vol. 72, No. 6
0019-9567/04/$08.00+0 DOI: 10.1128/IAI.72.6.3592–3603.2004

Legionella dumoffii DjlA, a Member of the DnaJ Family, Is Required for Intracellular Growth

Hiroko Ohnishi,[1,2] Yoshimitsu Mizunoe,[1]* Akemi Takade,[1] Yoshitaka Tanaka,[3] Hiroshi Miyamoto,[4] Mine Harada,[2] and Shin-ichi Yoshida[1]

Department of Bacteriology[1] and Department of Medicine and Biosystemic Science, Internal Medicine,[2] Faculty of Medical Sciences, and Division of Pharmaceutical Cell Biology, Graduate School of Pharmaceutical Sciences,[3] Kyushu University, Fukuoka 812-8582, and Department of Microbiology, School of Medicine, University of Occupational and Environmental Health, Kitakyushu 807-8555,[4] Japan

Received 12 November 2003/Returned for modification 5 January 2004/Accepted 10 February 2004

***Legionella dumoffii* is one of the common causes of Legionnaires' disease and is capable of replicating in macrophages. To understand the mechanism of survival within macrophages, transposon mutagenesis was employed to isolate the genes necessary for intracellular growth. We identified four defective mutants after screening 790 transposon insertion mutants. Two transposon insertions were in genes homologous to *icmB* or *dotC*, within *dot/icm* loci, required for intracellular multiplication of *L. pneumophila*. The third was in a gene whose product is homologous to the 17-kDa antigen forming part of the VirB/VirD4 type IV secretion system of *Bartonella henselae*. The fourth was in the *djlA* (for "*dnaj*-like *A*") gene. DjlA is a member of the DnaJ/Hsp40 family. Transcomplementation of the *djlA* mutant restored the parental phenotype in J774 macrophages, A549 human alveolar epithelial cells, and the amoeba *Acanthamoeba culbertsoni*. Using confocal laser-scanning microscopy and transmission electron microscopy, we revealed that in contrast to the wild-type strain, *L. dumoffii djlA* mutant-containing phagosomes were unable to inhibit phagosome-lysosome fusion. Transmission electron microscopy also showed that in contrast to the virulent parental strain, the *djlA* mutant was not able to recruit host cell rough endoplasmic reticulum. Furthermore, the stationary-phase *L. dumoffii djlA* mutants were more susceptible to H_2O_2, high osmolarity, high temperature, and low pH than was their parental strain. These results indicate that DjlA is required for intracellular growth and organelle trafficking, as well as bacterial resistance to environmental stress. This is the first report demonstrating that a single DjlA-deficient mutant exhibits a distinct phenotype.**

Legionella dumoffii was first isolated from cooling-tower water in 1979 (18) and later from a postmortem lung specimen in the same year (40) as an atypical *Legionella*-like organism. It was later classified by Brenner (11) as a new species, *L. dumoffii*. *Legionella* species are gram-negative, facultative intracellular parasites of freshwater amoebae in nature and are capable of growing within alveolar macrophages and epithelial cells after being accidentally transmitted to humans (22). The most common human pathogen in the genus *Legionella* is *L. pneumophila*, the causative agent of Legionnaires' disease (71). Humans contract the disease from contaminated environmental sources, primarily by aspiration of aerosolized water sources (22). After internalization by alveolar macrophages, *L. pneumophila*-containing phagosomes do not acidify (34) or fuse with lysosomes (33). Instead, the mitochondria, smooth vesicles, and rough endoplasmic reticula (RER) near these *L. pneumophila*-containing vacuoles are recruited, and *L. pneumophila* begins to multiply in this unique niche (32). This altered endocytic pathway is considered to be controlled by the Dot/Icm type IV protein secretion system (5, 17, 48, 55, 56, 74). The *dot/icm* genes are essential for the intracellular growth of *L. pneumophila* (5, 51, 60). The presence of the *dot/icm* loci in several species of *Legionella* was shown by Southern or PCR analysis (4, 36, 43); however, the contributions of these loci to the pathogenesis of other species have yet to be investigated.

L. dumoffii is the fourth or fifth most common pathogen causing Legionnaires' disease (8, 71). Some of proteins or factors which may promote *L. pneumophila* pathogenesis, such as flagella, catalase, and gelatinase, are also present in *L. dumoffii*. Several putative virulence factors—lipase, oxidase, and a zinc metalloprotease—are absent in *L. dumoffii* (6, 11, 52). *L. dumoffii* is capable of infecting and replicating within Vero cells and the human lung alveolar epithelial cell line A549 in vitro (41, 42). To elucidate the molecular mechanisms of the intracellular growth of this organism, we attempted to isolate the mutants that exhibited defective growth phenotypes in J774 mouse macrophage-like cells and A549 human type II alveolar epithelial cells by using transposon mutagenesis. We isolated four clones attenuated in virulence within mammalian cells by screening 790 derivatives with Tn*903*dII*lacZ* insertions. Two of four genes flanking the transposon insertions encode the proteins homologous to *L. pneumophila* IcmB and DotC (5, 51, 60), respectively. One gene has similarity to *virB5* (17-kDa antigen) in the VirB/VirD4 type IV secretion system of *Bartonella henselae* (14, 49, 59). The deduced protein encoded by a fourth gene showed homology to DjlA proteins (16). The DjlA homologue, a member of the DnaJ/Hsp40 family, was originally identified in *Escherichia coli* as a product of a hypothetical open reading frame (13, 72), and since then homologues have been identified in many other bacterial species, such as *Coxiella burnetti* (73), *Salmonella enterica* serovar Ty-

* Corresponding author. Mailing address: Department of Bacteriology, Faculty of Medical Sciences, Kyushu University, Fukuoka 812-8582, Japan. Phone: 81-92-642-6128. Fax: 81-92-642-6133. E-mail: ymizunoe@bact.med.kyushu-u.ac.jp.

TABLE 1. Bacterial strains and plasmids used in this study

Strain or plasmid	Relevant characteristics	Source or reference
Strains		
E. coli		
DH5α	F⁻*endA1 hsdR17 supE44D thi-1 recA1*Δ(*argF-lacZYA*)*U169*(ϕ80δ *lacZM15*) *gyrA96*λ⁻	30
VCS257	DP50 *sup* F[*supE44 supF58 hsd53*(r_B m_B) *dapD8 lacY1 gln*V44 Δ(*gal-uvrB*)47 *tyrT58 gyrA29 tonA53* Δ(*thyA57*)]	Stratagene
L. dumoffii Tex-KL		ATCC 33343
HOLD254	Tex-KL *djlA*::Tn*903*dII*lacZ*	This study
HOLD491	Tex-KL *icmB*(*dotO*)::Tn*903*dII*lacZ*	This study
HMLD4001	Tex-KL 17-kDa antigen::Tn*903*dII*lacZ*	This study
HMLD4002	Tex-KL *dotC*::Tn*903*dII*lacZ*	This study
HOLD254-1	Tex-KL *djlA*::Tn*903*dII*lacZ*/pHRO18	This study
HOLD254-2	Tex-KL *djlA*::Tn*903*dII*lacZ*/pHRO25	This study
Plasmids		
pGEM-T Easy	Amp^r, *lacZ*, general cloning vector	Promega
pUC19	Amp^r, parental cloning vector	70
pBR322	*ori*R (ColE1); Amp^r Tc^r	New England Biolabs
pHC79	Wide-host-range pBR322 origin cosmid vector; Amp^r Tc^r	31
pLAW317	*rpsL* MCS[a] *oriT*(RK2) Cm^r*loxP ori*R(ColE1) Amp^r*loxP*	68
pLAW330	pLAW317::Tn*903*dII*lacZ tnpA*(Tn*903*) *oriR*(f1)	68
pMMB207	RSF1010 derivative, *lncQ lac* I^q Cm^r P*tac oriT*	47
pMMB207c	pMMB207 with 8-bp insertion in *mobA*; Mob	45
pHRO1	Tn*903*dII*lacZ*-containing HindIII fragment from HOLD254 in pBR322	This study
pHRO2	Tn*903*dII*lacZ*-containing BamHI fragment from HOLD491 in pBR322	This study
pHRO3	Tn*903*dII*lacZ*-containing HindIII fragment from HMLD4001 in pBR322	This study
pHRO4	Tn*903*dII*lacZ*-containing HindIII fragment from HMLD4002 in pBR322	This study
pHRO17	Amp^r; 4-kbp ScaI-EcoRI fragment containing *djlA* gene in pUC19	This study
pHRO18	4-kbp Pst-EcoRI fragment containing *djlA* from pHRO17 in pMMB207c	This study
pHRO24	PCR fragment of *djlA* cloned into pGEM-T Easy vector	This study
pHRO25	EcoRI-PstI fragment (1,155 bp) containing *djlA* from pHRO24 cloned into pMMB207c	This study

[a] MCS, multiple-cloning site.

phimurium, *Klebsiella pneumoniae*, and *Vibrio cholerae*. DjlA carries the J-domain characteristic of the DnaJ/Hsp40 family and is essential for interaction with the Hsp70 homologue, DnaK, by increasing its ATPase activity (67). Overproduction of DjlA stimulates colanic acid production in *E. coli* (15, 16, 27, 73). Analysis of the DjlA null mutant demonstrated that the gene was not essential for viability (16). Although DjlA homologue is present in *L. pneumophila* (10), the role of this gene in pathogenesis has yet to be determined.

In this study, we investigated the role of the *djlA* gene in avoidance of fusion with lysosomes and its role in organelle trafficking within macrophages and in bacterial resistance to environmental stresses such as oxidative products, high temperature, high salt concentrations, and acidic pH.

MATERIALS AND METHODS

Bacterial Strains, plasmids, and media. The bacterial strains and plasmids used in this work are described in Tables 1 and 2. The *L. dumoffii* Tex-KL strain and its derivatives were grown on buffered charcoal-yeast extract (BCYE) agar plates or in buffered yeast extract (BYE) broth. BYE broth was based on the formation of BCYE, but the charcoal and agar were omitted. *E. coli* DH5α (Toyobo Co., Ltd., Osaka, Japan) was used for the majority of the cloning experiments. As required, antibiotics were used at the following concentrations: kanamycin (KM), 30 μg/ml; chloramphenicol (CM), 5 or 20 μg/ml (for *L. dumoffii*); KM, 30 μg/ml; ampicillin (AMP), 50 μg/ml; CM, 20 μg/ml (for *E. coli*).

Cell culture. J774A.1 macrophages (JCRB9108), refered to as J774 in this paper, were derived from mouse macrophage-like cells. The cell line A549 (JCRB0076) was donated by the Health Science Research Resources Bank, Osaka, Japan. The cells were established from a human alveolar epithelial carcinoma and have characteristics of well-differentiated type II pneumocytes. J774 cells and A549 cells were cultured in RPMI 1640 medium (GIBCO, Grand Island, N.Y.) supplemented with 10% fetal bovine serum (FBS; Dainippon

TABLE 2. Strains of *Legionella* species used and their clinical relevance

Legionella strain	Source	Clinical relevance
L. pneumophila serogroup1 (ATCC 33153)	Human	Yes
L. pneumophila serogroup6 (ATCC 33215)	Human	Yes
L. dumoffii (ATCC 33343)	Human	Yes
L. longbeachae (ATCC 33462)	Human	Yes
L. micdadei (ATCC 33218)	Human	Yes
L. bozemanii (ATCC 33217)	Human	Yes
L. feelei (ATCC 35849)	Human	Yes
L. gormanii (ATCC 33297)	Soil	Yes
L. jordanis (ATCC 33623)	Water	Yes
L. quinlivanii (ATCC 43830)	Water	No
L. moravica (ATCC 43877)	Water	No
L. gratiana (ATCC 49413)	Water	No
L. geestiana (ATCC 49504)	Water	No
L. rubrilucens (ATCC 35304)	Water	No
L. worsleiensis (ATCC 49508)	Water	No
L. jamestowniensis (ATCC 35298)	Soil	No
L. adelaidensis (ATCC 49625)	Water	No

Pharmaceutical, Osaka, Japan). *Acanthamoeba culbertsoni* (44) was propagated at 28°C in 25-cm^2 flasks (Falcon) containing 8 ml of peptone yeast extract glucose (PYG) and AC buffer (PYG + AC) (9, 46).

DNA manipulation. Restriction enzymes and T4 DNA polymerase were purchased from Takara Shuzo Co., Ltd. (Kyoto, Japan) and Toyobo Co., Ltd. (Osaka, Japan). Calf intestine alkaline phosphatase was purchased from New England Biolabs Inc. (Beverly, Mass.). PCR amplification was performed by using The Ready To Go PCR-Beads (Amersham Pharmacia Biotech, Piscataway, N.J.) or Ex-Taq polymerase (Takara, Kyoto, Japan). Oligonucleotides used for PCR amplification were purchased from Japan Flour Co., Ltd. (Tokyo, Japan). Plasmid DNA was isolated from *E. coli* and *L. dumoffii* by using the Wizard Plus Mini Prep (Promega, Madison, Wis.) or the alkaline lysis method (58). Chromosomal DNA of *L. dumoffii* was purified using the Genomic Prep cells and tissue DNA isolation kit (Amersham Pharmacia Biotech). Electroporations were performed with a Bio-Rad Gene Pulser, as recommended by the manufacturer. Purification of DNA fragments from agarose gels for subcloning or labeling was carried out with a GFX PCR DNA and gel band purification kit (Amersham Pharmacia Biotech).

Transposon mutagenesis and construction of a bank of mutants. *L. dumoffii* was mutated with the Tn*903* derivative Tn*903*dII*lacZ*, as described previously (68). Tn*903*dII*lacZ* confers KM resistance (Km^r) and contains a 5′-truncated *lacZ* gene. Briefly, after electroporation of plasmid pLAW330, containing Tn*903*dII*lacZ*, into *L. dumoffii* Tex-KL, bacteria were incubated in BYE broth for 5 h at 37°C and plated onto BCYE-KM plates. Km^r transformants containing β-galactosidase activity were identified as blue colonies after the the plates were overlaid with 0.8% agar containing 0.6 mg of 5-bromo-4-chloro-3-indolyl-β-D-galactoside (X-Gal) per ml. Km^r Cm^s colonies were saved as simple Tn*903*dII*lacZ* insertion mutants of *L. dumoffii*.

Southern hybridization. Chromosomal DNA from *L. dumoffii* strains was digested with HindIII, resolved on a 0.7% agarose gel in TBE buffer, and blotted onto a nylon membrane. DNA probes were prepared by random-primed labeling with digoxigenin-1 1-dUTP. The methods for prehybridization and hybridization and the washing conditions were the same as described previously (58), and the procedure for colorimetric detection of hybridized DNA was performed using the digoxigenin system (Roche Diagnostic Co., Indianapolis, Ind.).

Cloning and sequencing of the chromosomal junction of Tn*903*dII*lacZ* insertion in the mutants. Genomic DNA from the *L. dumoffii* mutants was digested with HindIII or BamHI and ligated to HindIII- or BamHI-digested pBR322. The ligation was used to transform DH5α, and the transformation mixture was plated on Luria-Bertani agar plates containing KM and AMP. Plasmid DNA was extracted, and the regions flanking Tn*903*dII*lacZ* were sequenced with the *lacZ* primer (5′-CCCAGTCACGACGTTG-3′) and the Km^r primer (5′-AATTTAA TCGCGGCCTCGAG-3′), corresponding to the 5′ and 3′ ends, respectively, of Tn*903*dII*lacZ*.

Construction of plasmids for complementation. For wild-type *L. dumoffii* genomic library construction, the genomic DNA was isolated from *L. dumoffii* and partially digested with Sau3 AI, and fragments of about 40 kb were purified. The fragments were ligated to the BamHI-digested, calf intestinal alkaline phosphatase-treated cosmid vecter pHC79 (31). The ligation products were packaged, in vitro, using the GigapackII Gold packaging system (Stratagene). Packaged hybrid cosmids were then used to infect *E. coli* strain *VCS257*. Recombinant clones were screened for the presence of a 1,085-bp PCR product (254-45), amplified using primers 254-4 (5′-GCTTCTTCCTTTCCACCATAA-3′) and 254-5 (5′-AGGTAGGCCTTGGGCAATTA-3′), by colony hybridization techniques. The probes used for colony hybridization were labeled with the digoxigienin random-primed DNA-labeling system (Roche). About 1,000 recombinant clones from the library were plated on the Luria-Bertani–plus-AMP plates for screening. Several positive cosmid clones were identified. The 4-kb ScaI-EcoRI fragment containing 254-45 from one of these cosmid clones was cloned into HincII-EcoRI-digested pUC19 to generate pHRO17. The recombinant clone was confirmed to contain 254-45 by Southern blot hybridization. The 4-kb PstI-EcoRI fragment from pHRO17 was cloned into shuttle vecter pMMB207c digested with PstI and EcoRI to generate pHRO18. pMMB207c is a nonmobilizable derivative of pMMB207 containing an 8-bp insertion within the *mobA* gene (at base 3325) and replicates stably in *Legionella* spp. (45). pHRO18 was electroporated into HOLD254 to yield the complemented strain *HOLD254-1*. The DNA fragment containing the *djlA* gene was PCR amplified from plasmid pHRO17 by using primer pair djlA-1-EcoRI (5′-GGGAATTCGAGTAGATA CGAAGCAGGGT-3′) and djlA-2-PstI (5′-GGCTGCAGTTCCACCATAAAC GGACTACA-3′). EcoRI and PstI sites (underlined sequences) were incorporated into these primers, respectively. The 1,155-bp PCR product that was generated contained 158 bp upstream of the ATG codon of *djlA* and 72 bp downstream of the stop codon of *djlA*. This PCR product was ligated into the pGEM-T Easy vector (Promega), resulting in pHRO24. The 1,155-bp EcoRI-PstI fragment from pHRO24 was then cloned into EcoRI-PstI-digested pMMB207c, creating pHRO25. The *djlA* mutant of *L. dumoffii*, HOLD254, was transformed with pHRO25 by electroporation. One of the transformants containing the desired plasmid was designated HOLD254-2. The cloned *djlA* gene was sequenced by using the primer within pMMB207c (pMMB207c-1; 5′-GTG TGGAATTGTGAGCGGAT-3′) and the primer within the *djlA* gene (254-3; 5′-GCTGATGGGCTGGATAGCAA-3′).

DNA sequence analysis of the region surrounding the *djlA* gene. Primer pair djlA-3 (5′-AAGGATGGTAACTCTGACTCT-3′) and pHC79-2 (5′-TTGGAG CCACTATCGACTAC-3′) within the *djlA* gene and pHC79, respectively, were used to amplify the flanking region of the *djlA* gene from the cosmid clone containing *djlA* gene. This 4-kb PCR product and the 4-kb plasmid DNA within pHRO17 were sequenced using a primer walking technique. DNA-sequencing reactions were performed on plasmid templates with the CEQ DTCS-Quick Start kit (Beckman Coulter, Inc., Fullerton, Calif.) and the CEQ DNA analysis system (Beckman Coulter, Inc.). The nucleotide sequences and deduced amino acid sequences were compared to the GenBank database by using the programs BLASTX and BLASTP and also to the incomplete genomic database of *L. pneumophila* Philadelphia I (http://genome3.cpmc.columbia.edu/~legion/ngnp1033033). Motif searches were carried out using the Prosite program.

Intracellular growth assay. Growth of *L. dumoffii* in J774 cells and A549 cells was determined by using a previously described standard intracellular growth assay (43, 74). *L. dumoffii* strains were grown in BYE broth to the early stationary phase. Approximately 2×10^9 bacteria were pelleted, resuspended, and diluted (1:1,000) in RPMI 1640 tissue culture medium. The bacteria were then added to J774 cells and A549 cells (2×10^5 per well) in 24-well dishes to give a multiplicity of infection (MOI) of about 10. The infected cells were incubated at 37°C under 5% CO_2–air for 1.5 h and washed three times with phosphate-buffered saline (PBS) to remove extracellular bacteria. To measure bacterial internalization, 1 ml of sterile distilled H_2O was added to the wells to release intracellular bacteria from the host cells, and CFU were determined by plating dilutions on BCYE agar plates. To each of the remaining wells, 0.5 ml of fresh tissue culture medium was added. At 24-h intervals, the intracellular and extracellular bacteria in each well were combined, and the total CFU was determined by plating the dilutions onto BCYE agar plates. Infection of *A. culbertsoni* was carried out in an almost identical manner, except that bacteria were suspended in AC buffer and 0.05% Triton X-100 was added to release intracellular bacteria.

Assessment of phagosome-lysosome fusion by confocal microscopy. *L. dumoffii* strains were grown overnight to saturation at 37°C in BYE broth. They were added at an MOI of 25 to 50 to 8×10^4 J774 cells on glass coverslips in 24-well tissue culture plates. The plates were centrifuged at $150 \times g$ for 5 min at room temperature and incubated for 20 min in 5% CO_2–air at 37°C. Extracellular bacteria were removed by washing three times with PBS, and fresh tissue culture medium was added to each well. The plates were returned to the incubator for 4 h. Cells were fixed for 15 min at room temperature in P-PFA (4% paraformaldehyde in 1 × PBS [pH 7.4]) (43, 74). Coverslips were immersed in PBS–0.1% Saponin for 5 min to permeabilize the cells and blocked with 5% FBS in PBS for 5 min. Lysosomes and late endosomes were stained with rat monoclonal antibody 1 D4B (1:100) specific for LAMP-1 or Ab1 93 (1:100) specific for LAMP-2, and the bacteria were stained with rabbit anti-*L. dumoffii* polyclonal antibody (1: 10,000) for 1 h. The cells were washed with blocking solution three times and incubated for 30 min with Cy3-labeled goat anti-rat secondary antibody (1:300) and Alexa488-labeled goat anti-rabbit secondary antibody (1:300). The coverslips were then washed three times with blocking solution. All antibody dilutions were performed with PBS containing 0.5% FBS and 0.1% Saponin. Coverslips were inverted onto 1 μl of mounting medium (50% glycerol) on glass slides (39). Fluorescence was viewed using a Radiance 2100 MP confocal microscope (Bio-Rad Laboratories, Richmond, Calif.). Alexa488- and Cy3-labeled secondary antibodies were purchased from Molecular Probes (Eugene, Oreg.). Rat monoclonal antibodies to LGP107 (mouse LAMP-1) and LGP96 (mouse LAMP-2) were purified from mouse liver lysosomal membranes, as described previously (23).

Quantification of phagosome-lysosome fusion by electron microscopy. To label cell lysosomes, J774 macrophages were incubated with bovine serum albumin (BSA)-conjugated colloidal 15-nm-diameter gold particles (BSA-gold) overnight, chased for 3 h, and pulsed with stationary-phase *L. dumoffii* strains at an MOI of 50 (19, 33). At 4 h postinfection, the cells were fixed and processed for electron microscopy as previously described (66). Briefly, infected macrophages were fixed with 2% glutaraldehyde and then with 1% OsO_4, dehydrated with ethanol, and embedded in Epon. Ultrathin sections were stained with uranyl

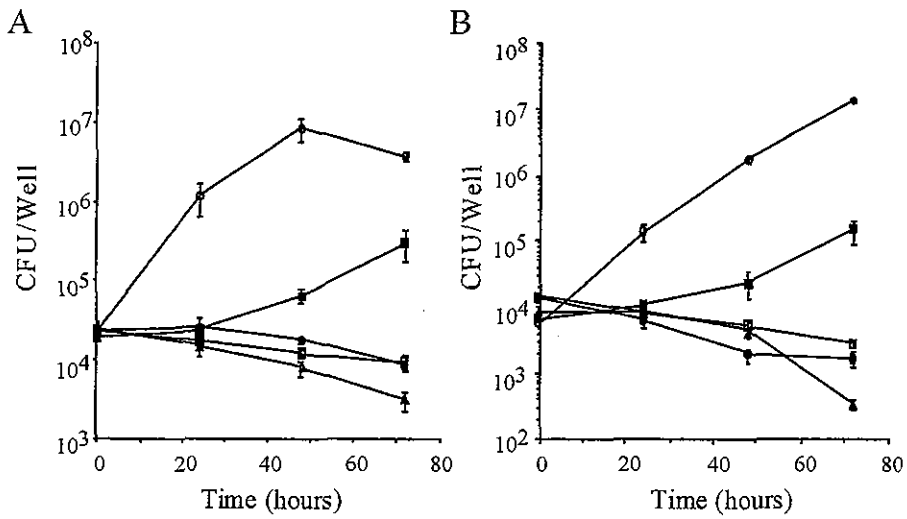

FIG. 1. Intracellular growth of *L. dumoffii* strains within J774 mouse macrophages (A) and A549 human epithelial cells (B). The formation of colonies (CFU per milliliter) was determined at the times indicated, in triplicate, for at least two independent experiments. Error bars indicate the standard deviations determined from samples taken from one experiment. Symbols: ○, *L. dumoffii* wild-type strain; ■, HOLD254; □, HOLD491; ●, HMLD4001; △, HMLD4002.

acetate followed by lead citrate and examined by electron microscopy in a JEM 2000EX instrument (JEOL, Ltd., Tokyo, Japan).

Examination of RER recruitment by transmission electron microscopy. J774 cells were plated in 90-mm-diameter petri dishes (2×10^5 cells/ml) and infected with stationary-phase *L. dumoffii* strains at an MOI of 20 for 8 and 24 h (32). Ultrathin sections were prepared as described above.

Assays for survival under stress conditions. *L. dumoffii* strains were grown for 2 to 3 days on BCYE agar plates and used to inoculate 4 ml of BYE medium. The bacteria were then grown at 37°C with aeration for at least 16 h. The initial CFU count was about 10^{10} per ml. Cells were divided into aliquots, centrifuged, and resuspended in equal volumes of 1 × M63 salts [22.0 mM KH_2PO_4, 40.2 mM K_2HPO_4, 14.6 mM $(NH_4)_2SO_4$ 500 nM $FeSO_4$ (pH6.5)]. One aliquot was used for measuring the untreated CFU. For heat shock, aliquots were transferred to 48°C and incubated for 60 min. For oxidative stress, aliquots were exposed to 10 mM H_2O_2 for 30 min. For osmotic shock, aliquots were exposed to 5 M sodium chloride for 30 min. For acid shock, aliquots were resuspended in 0.1 M citric acid (pH 3) for 5 min. Except for heat stress, the cells were incubated in a 37°C heat block. At the indicated time points, the cells were washed with 1 × M63 salts and serially diluted to determine the CFU on BCYE agar plates (29).

Detection of a *djlA* gene in other *Legionella* spp. The presence of *djlA* in 17 different strains of *Legionella* spp. was examined by PCR with the primer pair djlA-cons-1 (5′-ATAACAACCTGGTGGGGAAA-3′) and djlA-cons-2 (5′-TG GGCAATTAATTTATCTGGATG-3′), located in the transmembrane domain (TMD) and J domain within the *djlA* gene, respectively, which gave a 791-bp product. PCR was carried out by using chromosomal DNA from BCYE plate-grown bacteria as a template.

RESULTS

Isolation of intracellular growth mutants. Wild-type *L. dumoffii* Tex-KL was mutagenized with Tn*903*dII*lacZ* as described previously (57, 68). Plasmid pLAW330 containing Tn*903*dII*lacZ* was introduced into *L. dumoffii*, and 790 Km^r Cm^s mutants of *L. dumoffii* (HOLD strains 1 to 656 and HMLD strains 4004 to 4044 and 4048 to 4140) with various levels of β-galactosidase activity were isolated. The 790 mutants were individually screened for their ability to kill mouse macrophage-like J774 cells and human alveolar epithelial A549 cells. The mutants were grown for 2 days in 96-well tissue culture plates containing BYE medium. Then 5-μl samples of 2-day-old cultures of mutants were transferred to another 96-well tissue culture plate containing J774 cells or A549 cells. At each 24-h time point after infection, the monolayers were visually examined to determine the extent of killing of both J774 cells and A549 cells. From several assays, we isolated five mutants, based on their reproducible phenotypes. Southern blot analysis of the HindIII-digested genomic DNA of each of the five mutants probed with pLAW330 showed that four of them contained a single copy of the Tn*903*dII*lacZ* insertion and that these insertions were distributed in distinct locations within the chromosome of *L. dumoffii* (data not shown). For reasons not yet understood, one of the mutants showed no hybridization. Therefore, the four strains were chosen for further analysis. In vitro, the growth of these four mutants in BYE broth and on BCYE agar plates was similar to that of the wild-type strain (data not shown).

Intracellular growth phenotype of the mutants within J774 macrophages and alveolar epithelial cells. We examined the four candidates for their capacity to survive and to replicate within J774 macrophages and A549 epithelial cells. Bacterial CFU were determined over 3 days. The wild-type strain multiplied over 100-fold during the 3-day incubation period within J774 macrophages (Fig. 1A). HOLD254 showed a 1-log-unit increase after 3 days of incubation, whereas HOLD491, HMLD4001, and HMLD4002 did not grow during the incubation period in J774 cells. Within A549 epithelial cells (Fig. 1B), the wild-type strain increased approximately 1,000-fold over the 3-day period, while there was a 10-fold increase in the number of intracellular bacteria of HOLD254 over 3 days. For HOLD491 and HMLD4001, the number of CFU after 3 days of infection decreased 1 log unit to the initial number of CFU, and HMLD4002 was severely defective in intracellular survival (Fig. 1B).

Sequence analysis of the junctions of Tn*903*dII*lacZ* insertions. We cloned the HindIII fragment containing the Tn*903*dII*lacZ* insert and the flanking sequences of the mutants (HOLD254, HOLD491, HMLD4001, and HMLD4002). Using

TABLE 3. Sequence similarities of *L. dumoffii* genes responsible for intracellular multiplication[a]

Mutant strain	Homologous gene	Organism	% Identity	% Positive
HOLD254	*djlA*	*Legionella pneumophila*	61	73
HOLD491	*icmB/dotO*	*Legionella pneumophila*	89	95
HMLD4001	17-kDa antigen gene	*Bartonella henselae*	26	43
HMLD4002	*dotC*	*Legionella pneumophila*	85	92

[a] The values are taken from a Basic Local Alignment Search Tool for amino acid comparison (BLASTX program).

the primer within Tn*903*dII*lacZ*, we partially sequenced and analyzed them to identify the genes responsible for intracellular multiplication. The results are summarized in Table 3. Sequence homology searches against the Gen Bank database were done with these genes and corresponding proteins. HOLD254, HOLD491, and HMLD4002 contain insertions within the genes homologous to known *L. pneumophila* genes. The gene disrupted in HOLD254 is the *djlA* (for "*dnaJ*-like *A*") gene, encoding a member of the Hsp40 protein family, which has not been characterized in *L. pneumophila*. HOLD491 and HMLD4002 had a transposon insertion in their sequences similar to *icmB (dotO)* and *dotC*, respectively, identified as genes essential for intracellular growth in *L. pneumophila* (5, 51). HMLD4001 had an insertion within a gene whose product showed amino acid similarity to the 17-kDa antigen, VirB5, of *B. henselae*; the gene is located within the *virB* locus, which encodes a putative type IV secretion system together with the downstream *virD4* gene (14, 49, 59). Recently, Schulein and Dehio (59) also showed that VirB4 and VirD4, encoded by the *virB* and *virD4* loci of *B. tribucorum*, were required for establishing intraerythrocytic bacteremia.

Complementation of an *L. dumoffii djlA* mutant. DjlA is known to be a heat shock protein DnaJ/Hsp40 homologue. The virulence of the *djlA* mutant was compared with that of the wild-type strain and the *djlA*-complemented mutant in J774 macrophages, A549 epithelial cells, and *A. culbertsoni*. The *djlA* mutant showed only a 100-fold increase in intracellular replication within *A. culbertsoni* (Fig. 2C). As shown in Fig. 2, bacterial growth was fully restored in the complemented strains HOLD254-1 and HOLD254-2. The restoration of the wild-type-level of multiplication of the *djlA* mutant within these cells, achieved after complementation in *trans* with the cloned *djlA* gene, is proof of the important role of *djlA* in the intracellular growth of *L. dumoffii*.

Complete sequence and genetic structure of *djlA*. Figure 3A shows the organization around the *djlA* gene and the location of the Tn*903*dII*lacZ* insertion. The transposon insertion (Tn) was located in the J domain at the C terminus of the predicted protein, which was the defined feature of the DnaJ family of molecular chaperones (16, 27). Since the two genes (*waaA* and *orf1*) which flanked *djlA* were both oriented in the opposite direction from the *djlA*, we consider the *djlA* to be transcribed

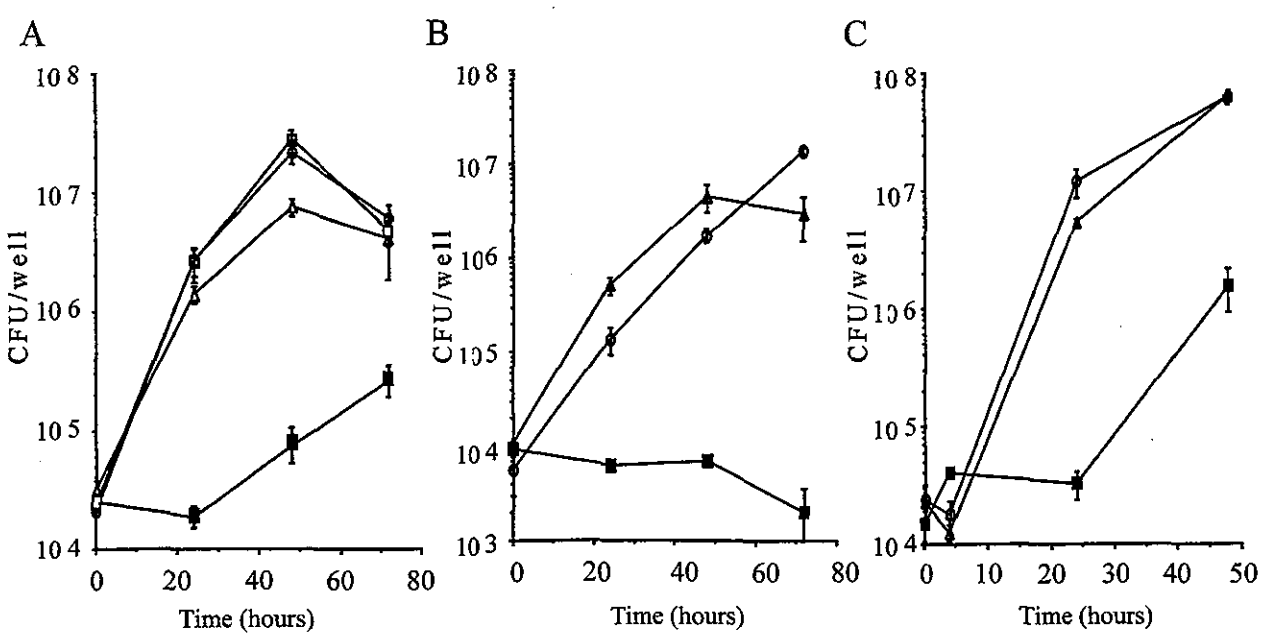

FIG. 2. Complementation of intracellular growth defects of *djlA* mutant HOLD254 in J774 macrophages (A), in A549 epithelial cells (B), and in *A. culbertsoni* (C). Growth was measured over 72 h (A and B) or 48 h (C). The data points and error bars represent the mean CFU/well for triplicate samples from a typical experiment (performed at least twice) and their standard deviations. Symbols: ○, *L. dumoffii* wild-type strain; ■, HOLD254; △, HOLD254-1 (*djlA*/pHRO18); □, HOLD254-2 (*djlA*/pHRO25).

monocistronically, and this transposon has no polar effect. The deduced amino acid sequence of *L. dumoffii* DjlA, together with *L. pneumophila* DjlA and *E. coli* DjlA, is presented in Fig. 3B. The putative *L. dumoffii djlA* gene encodes a protein of 302 amino acids with a predicted molecular mass of 35.33 kDa and an isoelectric point of 9.65. The protein size is similar to that of the *L. pneumophila* (296 amino acids) and *E. coli* (271 amino acids) proteins. *L. dumoffii* DjlA has 61% identity to *L. pneumophila* DjlA and 32% identity to *E. coli* DjlA (10, 16, 73). A potential TMD at the N terminus contains six glycines, spaced through the TMD at every three to five residues, which is similar to the structure of the TMD of *E. coli* (15, 16). There is a remarkable difference in the N terminus of DjlA protein between *E. coli* and *Legionella* spp. Clarke et al. (16) have demonstrated that *E. coli* DjlA is localized to the inner membrane and has a rare type III topology (i.e. N-out, C-in), with the N-terminal 6 to 8 residues located in the periplasm. *Legionella* spp. have longer stretches (15 residues) before the TMD structure, which are probably exposed in the periplasm. Another unique feature of *Legionella* DjlA is a glutamate-serine (QS)-rich spacer located before the J domain, instead of the glutamate-glycine (QG)-rich spacer of *E. coli* DjlA (Fig. 3B) (16). The cellular role of these QS- or QG-rich regions remain to be elucidated.

Quantification of endocytic maturation. To determine whether the *L. dumoffii* strains were able to inhibit endocytic maturation, we measured the colocalization of *L. dumoffii* phagosomes with endocytic markers LAMP-1 and LAMP-2. J774 macrophages were infected with postexponential phase *L. dumoffii* strains for 4 h (Fig. 4). The permeabilized cells were stained with monoclonal antibody 1D4B or Abl 93, specific for late endosomal and lysosomal proteins, LAMP-1 or LAMP-2. The *djlA* mutant was found in phagosomes that contained LAMP-1 (Fig. 4A), indicating that these vacuoles had fused with late endosomes, whereas, phagosomes containing wild-type *L. dumoffii* did not colocalize with LAMP-1 (Fig. 4A). When each *L. dumoffii* strain found in the phagosomes was scored for fusion with the late endosomal/lysosomal markers LAMP-1 and LAMP-2, approximately 80% of the wild-type bacteria were found in LAMP-1- and LAMP-2-negative phagosomes while 50 to 60% of the HOLD254 was found in LAMP-1- and LAMP-2-positive compartments (Fig. 4B). We also performed the same analysis for HOLD4002, the *dotC* mutant, and found that this mutant followed the same endocytic pathway as HOLD254, with 60 to 70% LAMP-1- and LAMP-2-positive (data not shown). We also conducted an assay of phagosome-lysosome fusion, at the ultrastructural level, using electron microscopy. BSA-gold was used as a pinocytic, fluid-phase marker of the endosomal-lysosomal pathway. BSA-gold was accumulated mainly in lysosomes after endocytosis of the conjugate-containing medium overnight at 37°C, followed by a chase period of 3 h at 37°C in conjugate-free medium as previously described (33). After a pulse with *L. dumoffii* strains and another chase for 4 h, electron microscopy counting of *L. dumoffii*-containing phagosomes that fused with BSA-gold-labeled lysosomes was performed to assess fusion (Fig. 5). Wild-type-strain-containing phagosomes did not fuse with BSA-gold-marked lysosomes (Fig. 5A). Quantitation showed that only 11.4% (24 of 210) of the phagosomes containing the wild-type strain fused with BSA-gold-marked lysosomes. On the other hand, 85% (187 of 220) of the phagosomes containing the *djlA* mutant strain accumulated BSA-gold (Fig. 5B). Thus, the *djlA* mutant was not able to evade phagosome-lysosome fusion.

Recruitment of the RER. In mammalian macrophages and protozoa, *L. pneumophila* replicates intracellularly in specialized vacuoles surrounded by the RER of the host cells (25, 32). To determine the intracellular location of *L. dumoffii*, we examined J774 macrophages infected with wild-type and *djlA* mutant *L. dumoffii* by using transmission electron microscopy. At 8 h postinfection, the RER around 61 (37.2%) of 164 phagosomes containing wild-type strains were recruited (Fig. 6A) whereas we could not find any phagosomes containing the *djlA* mutant surrounded by RER or attached directly by ribosomes (0 of 153 phagosomes). This was also the case at 24 h (Fig. 6B and data not shown). Phagosomes containing *djlA* mutant cells appeared to harbor much debris, resulting from fusing lysosomes with these vacuoles, while phagosomes containing wild-type cells did not have any contents other than replicating *L. dumoffii* cells (Fig. 6). At 24 h postinfection, many phagosomes containing wild-type cells were broken and their inhabiting macrophages were lysed (data not shown).

Susceptibility of the *djlA* mutant to stress stimuli. In eukaryotic host cells, intracellular pathogens encounter hostile conditions such as toxic oxygen or nitrogen derivatives, intraphagosomal acidification, and harsh degradative enzymes (54, 62). As mentioned above, *djlA* is essential for intracellular growth of *L. dumoffii*. Thus, we examined whether the *djlA* mutant has an increased susceptibility to different environmental stresses. Since previous publications (12, 29) had demonstrated that *L. pneumophila* induces stress resistance in the stationary phase, *L. dumoffii* strains were grown to the stationary phase in BYE medium and subjected to acid shock, oxidative stress, osmotic stress, and heat shock (pH 3 for 5 min, 10 mM H_2O_2 for 30 min, 5 M sodium chloride for 30 min, and 48°C for 60 min, respectively). Compared to the wild-type strain, there was an elevated susceptibility to all stress conditions of the *djlA* mutant strain. There was an increase in the sensitivity of the mutant of 9.8-, 7.4-, 2.6-, and 1.6-fold on exposure to oxidative stress, osmotic stress, heat shock, and acid shock, respectively (Fig. 7). These results suggest that DjlA participated in the protection of *L. dumoffii* on exposure to environmental stress. In the *djlA*-complemented strain, in contrast, resistance to all stress stimuli was restored. The variability in the degree of complementation may result from the different expression of genes from the plasmid and the chromosome.

Presence of *djlA* in other *Legionella* spp. To determine whether *djlA* is also present in nonpathogenic *Legionella* species, PCR amplification with primers in the *djlA* gene was performed for 17 different *Legionella* strains. All the strains used in this experiment are listed in Table 2. The expected 790-bp band was observed in all *Legionella* strains tested except *L. jordanis* and *L. adelaidensis*, irrespective of whether the strain was pathogenic (data not shown). Thus, *djlA* is not unique to particular *Legionella* strains.

DISCUSSION

Legionella spp. are facultative intracellular bacteria that overcome host cell defenses. Although many studies have been

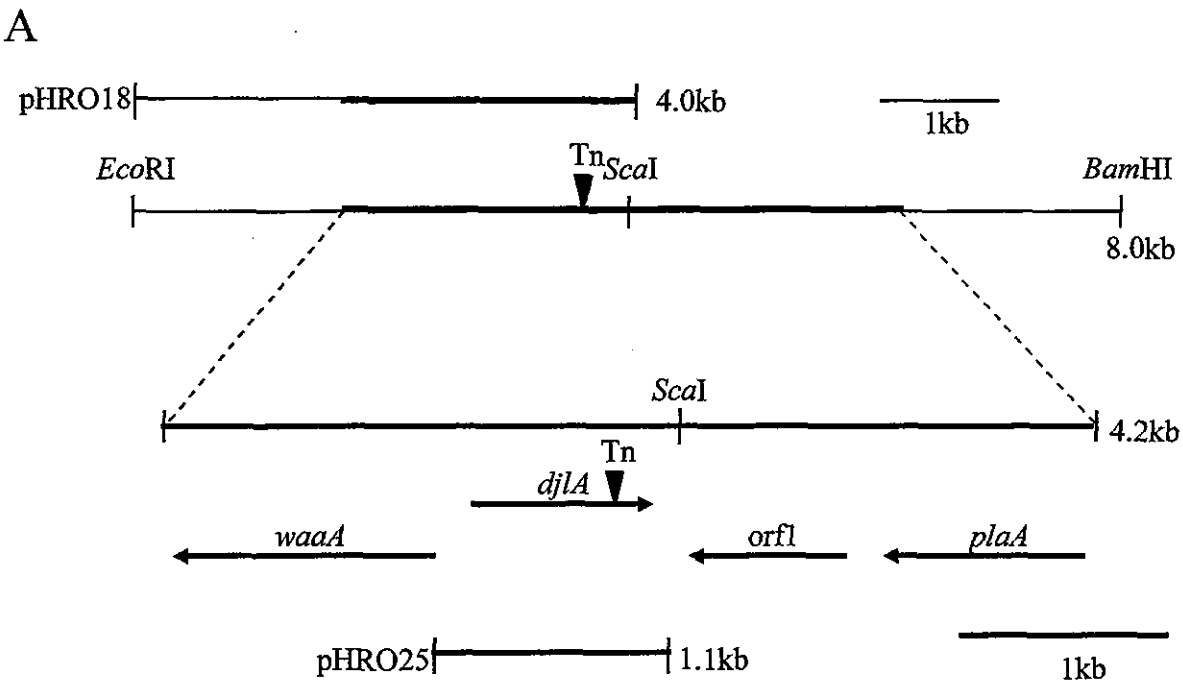

B

TMD

```
L. d MSLRDFFIITTWWGKIIGAFFGYLIAGPT-GAIFGLLVGNFFDRGLYNYFSNPHWLYYTEKRRAIQKIFFEA-TFLV 75
L. p MNLRDFFVITTWWGKILGAFFGYLTAGPV-GALFGILVGNFFDRGLVSYYSNPHWLYHAEKQRIVQKAFFEA-TFSI 75
E. c          MQYWGKIIGVAVALLMGGGFWGVVLGLLIGHMFDKAR----SRKMAWF-A-NQRERQ-AFF-ATTFEV 61

L. d MGHLAKADGRVSEQELDMAR-LFMDEMRLNGEQKTLAKHLFNEGKQSRFNLDSLLENLKKT--CKDNRDLLRLFI-D 148
L. p MGHVAKSDGRVSEQEISMAKSI-MNEMKLSKGQKDLAKRLFNEGKQADFNV-SL-ALIQLQRICKDNRDLLKLFV-D 148
E. c MGHLTKSKGRVTEADIHIASQL-MDRMNLHGASRTAAQNAFRVGKSDNYPLREKMRQ-FRSVCFGRFDLIRMFLEIQ 136

L. d IQYRAAQADG-LDSKKILLLDKIFSRLGFAPLHNQYRFYEDFGRSYSEPQYNTQEQP-QQSRQSQQSDSSSHSYSSY 223
L. p IQYRAAQVDG-LSSQKIHALDNIFTHLGFAPLHKQYRFYEDFG-SYFQQEQSKQHYHNQQEYKHT---SSSQG-QQG 219
E. c IQ--AAFADGSLHPNERAVLYVIAEELGI--SRAQFDQFLRMM----QGGAQFGGGYQQQT-------GGGNW-QQA 197
```

J-domain

```
L. d SRYNYQPTKNNMDYAFALLEVSPKASKQEVKKAYRRLLSRNHPDKLIAQGLPQEMIKMANEKTQKIVKAYELICESKGW 302
L. p YKP-QSPPNTLA-HAFALLEVSPNANKQEVRRAYRRLLSRNHPDKLIAQGLPEEMIKLANDKTHQIMKAYELICETKGWX 296
E. c QRG---P--TLE-DACNVLGVKPTDDATTIKRAYRKLMSEHHPDKLVAKGLPPEMMEMAKQKAQEIQQAYELIKQQKGFK 271
```

FIG. 3. Chromosomal arrangement of the region surrounding the *djlA* gene and sequence alignment of DjlA proteins. (A) At the top is a plasmid used for complementation studies (pHRO18) and an 8-kb region of the *L. dumoffii* cosmid clone including the *djlA* gene, along with the location of relevant restriction enzyme sites. The thick line represents the DNA region that we sequenced. Below these diagrams, the distance between the *djlA* gene and neighboring genes and the orientation and size of the transcribed genes are delineated by the arrows below the 4.2-kb sequenced region. Another plasmid used for complementation studies (pHRO25) is also shown. The site of the Tn*903*dIIlacZ insertion (Tn) is indicated by the inverted arrowhead. The full names of the gene mapped are as follows: *waaA*, Kdo transferase gene; *djlA*, *dnaJ*-like A gene; *plaA*, lysophospholipase A gene. Orf1 is a putative open reading frame which showed no homology to known genes. (B) Sequence similarity of the predicted DjlA protein of *L. dumoffii* (L.d, top line), *L. pneumophila* (L.p, middle line) and *E. coli* (E.c, bottom line). Amino acid residues conserved in the three sequences, appear in bold type. Gaps marked by dashes are introduced to reveal the maximal similarity among the sequences. The C-terminal J-domain and the N-terminal TMD are shown schematically above the sequences.

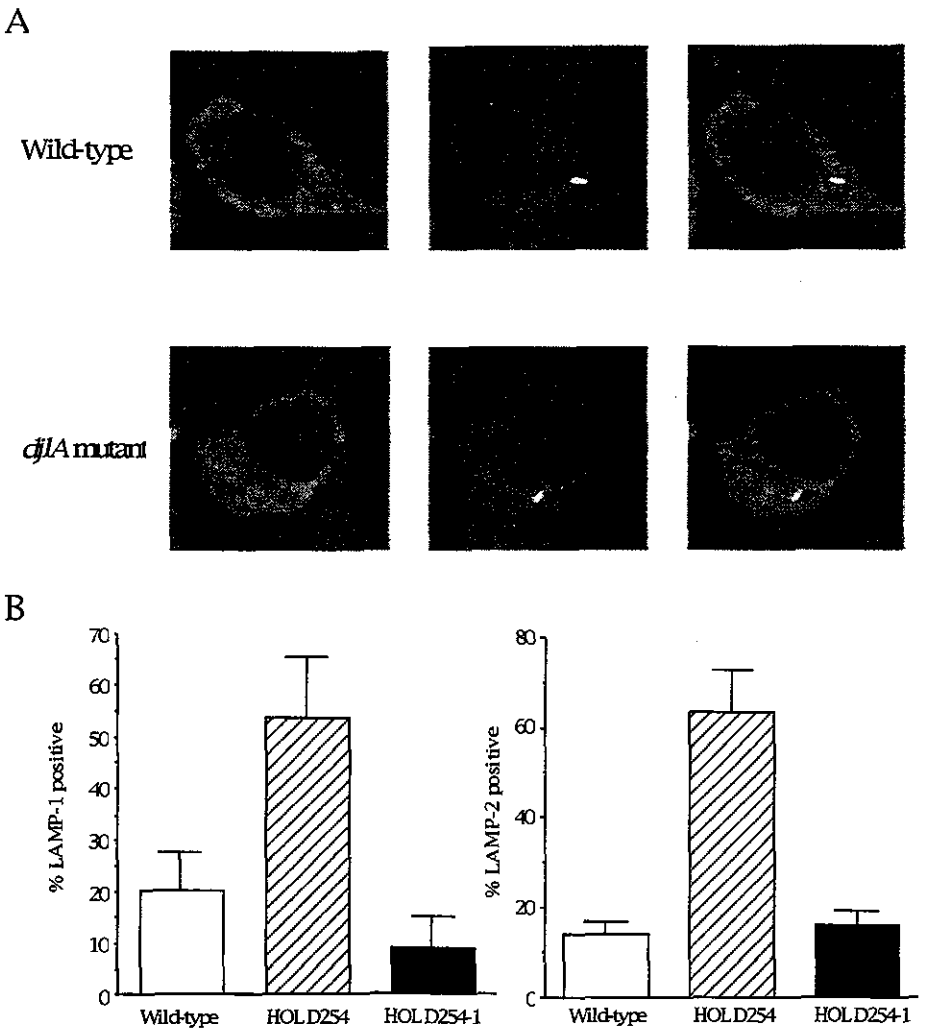

FIG. 4. Colocalization of the intracellular growth mutant with late endosomal/lysosomal marker LAMP-1 or LAMP-2 in J774 mouse macrophage cells by confocal laser-scanning microscopy. J774 macrophages were incubated with the *L. dumoffii* mutant or wild-type strain for 4 h. (A) Late endosomes and lysosomes stained with rat monoclonal antibody 1D4B, specific for LAMP-1, and Cy3-labeled anti-rat secondary antibody (red) are shown on the left. Bacteria stained with rabbit polyclonal antibody specific for *L. dumoffii* Tex-KL and Alexa488-labeled anti-rabbit secondary antibody (green) are shown in the middle. Merged images showing LAMP-1-positive bacteria (yellow) and LAMP-1-negative bacteria (green) are shown on the right. (B) Data were collected from about 100 intracellular bacteria in total. The percentage that is LAMP-1 or LAMP-2 positive was calculated by dividing the number of colocalizing intracellular bacteria by the total number of intracellular bacteria scored. The average and standard deviation described here were calculated from three coverslips per strain in two independent experiments.

undertaken to understand the intracellular life cycle of *L. pneumophila*, very few species other than *L. pneumophila* have been examined phenotypically. The aim of this study was to uncover how *L. dumoffii* survives and replicates in mammalian cells and to identify the genes of *L. dumoffii* needed for intracellular growth. We isolated 4 mutants that were defective in intracellular growth in macrophages and alveolar epithelial cells among 790 independently derived Tn*903*dII*lacZ* mutants of *L. dumoffii*. The defect in intracellular growth of these four mutants cannot be attributed to a defect in adherence or entry, because almost equal numbers of mutants and wild-type cells were present within mammalian cells at 0 h postinfection. Two of the four mutants had a transposon insertion in either the *dotC* or *icmB* homologues (5, 51, 60). The *dot/icm* genes are required for intracellular multiplication of *L. pneumophila* (5, 51, 60). Our results suggest that the *dotC* and *icmB* genes of *L. dumoffii* and *L. pneumophila* appear to perform similar functions. We propose that the *dot/icm* genes are involved in the pathogenesis of most *Legionella* species, since these genes are important in the intracellular growth of these distinct *Legionella* species.

One of the mutants defective in intracellular growth was shown to have a transposon insertion in the gene which had sequence similarity to the *djlA* gene (16). Cloning and sequence analysis of this gene revealed that the primary structure of *L. dumoffii* DjlA showed homology to other bacterial DjlA proteins (10, 16, 73). DjlA is the third DnaK cochaperone of *E. coli*, containing a J domain highly conserved in the DnaJ/

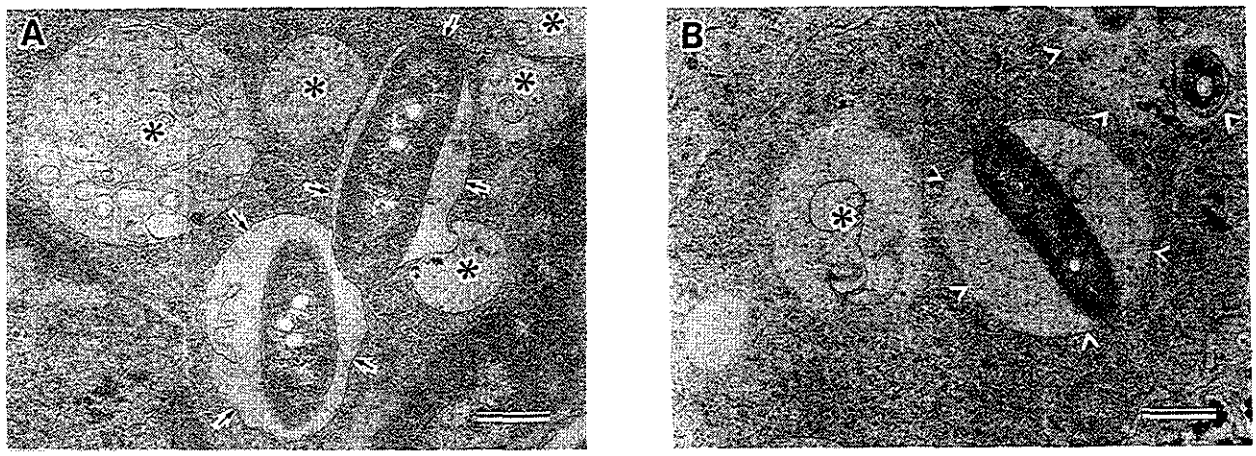

FIG. 5. Distribution of a lysosomal marker, BSA-gold, in phagosomes containing the wild-type strain or the *djlA* mutant strain. To label the lysosomal compartment, J774 cells were incubated with 15-nm BSA-gold overnight, washed, and then chased for 3 h. Cells were then infected with wild-type strain (A) or *djlA* mutant strain (B). At 4 h postinfection, the cells were fixed and processed for electron microscopy. Arrows in panel A indicate phagosomes containing no detectable gold; arrowheads in panel B indicate phagolysosomes containing BSA-gold; asterisks indicate, lysosomes containing BSA-gold. Bar, 0.5 μm.

Hsp40 family of molecular chaperones, including DnaJ and CbpA (16, 27, 65). CbpA is 39% identical to DnaJ along its entire length (64), while DjlA does not have any sequence similarity other than the J domain to DnaJ and CbpA in *E. coli* (26, 37). DjlA is unique in its structure and location in the DnaJ family. The J domain resides in the C terminus of DjlA but in the N terminus of other DnaJ family proteins. The N terminus of DjlA is integrated into the inner membrane through the single TMD, and the C-terminal J domain is located in the cytoplasm (16), while the whole of DnaJ and CbpA is localized in the cytoplasm. Moderate overproduction of *djlA* can trigger the synthesis of the colanic acid capsule in *E. coli*, mediated by the two-component regulatory system RcsC-RcsB, cooperating with DnaK and GrpE, but not DnaJ (15, 27, 37, 73). Unlike CbpA, DjlA could not adequately complement bacteriophage λ growth in a DnaJ-null background or restore bacterial growth above 40°C or below 16°C in the *dnaJ cbpA* null background in *E. coli* (15, 26, 37). The DjlA deletion mutant exhibits no apparent growth phenotype in *E. coli* (15, 16, 26). Thus, the true role of DjlA has been unclear.

We demonstrated that the *djlA* mutant of *L. dumoffii* exhibited a defective growth phenotype in mammalian cells and protozoan hosts. Phagosomes containing wild-type *L. dumoffii* excluded the late endosomal/lysosomal markers LAMP-1 and LAMP-2 and a lysosomal marker, BSA-gold, and were surrounded by RER in J774 macrophages, while *djlA* mutant-bearing phagosomes contained LAMP-1, LAMP-2, and BSA-gold and were not surrounded by RER (Fig. 4 to 6). It has been

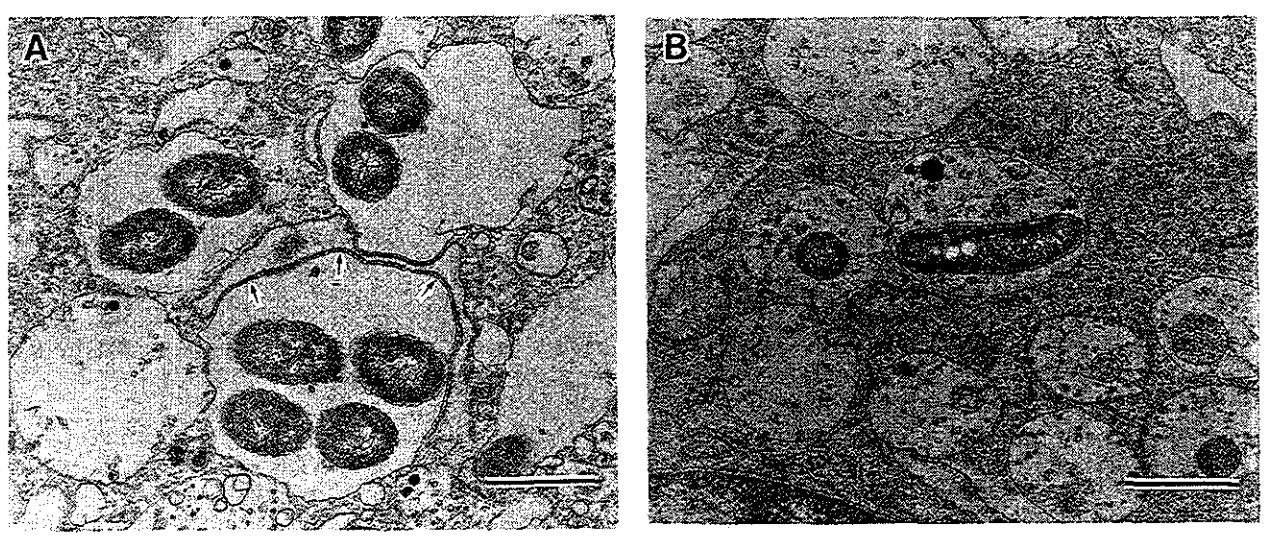

FIG. 6. Transmission electron micrographs of J774 mouse macrophages infected by the wild-type *L. dumoffii* (A) and the *djlA* mutant HOLD254 (B) at 8 h after infection. (A) Wild-type *L. dumoffii*-containing phagosomes were surrounded by RER (arrows). (B) HOLD254-containing phagosomes appeared to harbor much debris resulting from fusing lysosomes. Bar, 1.0 μm.

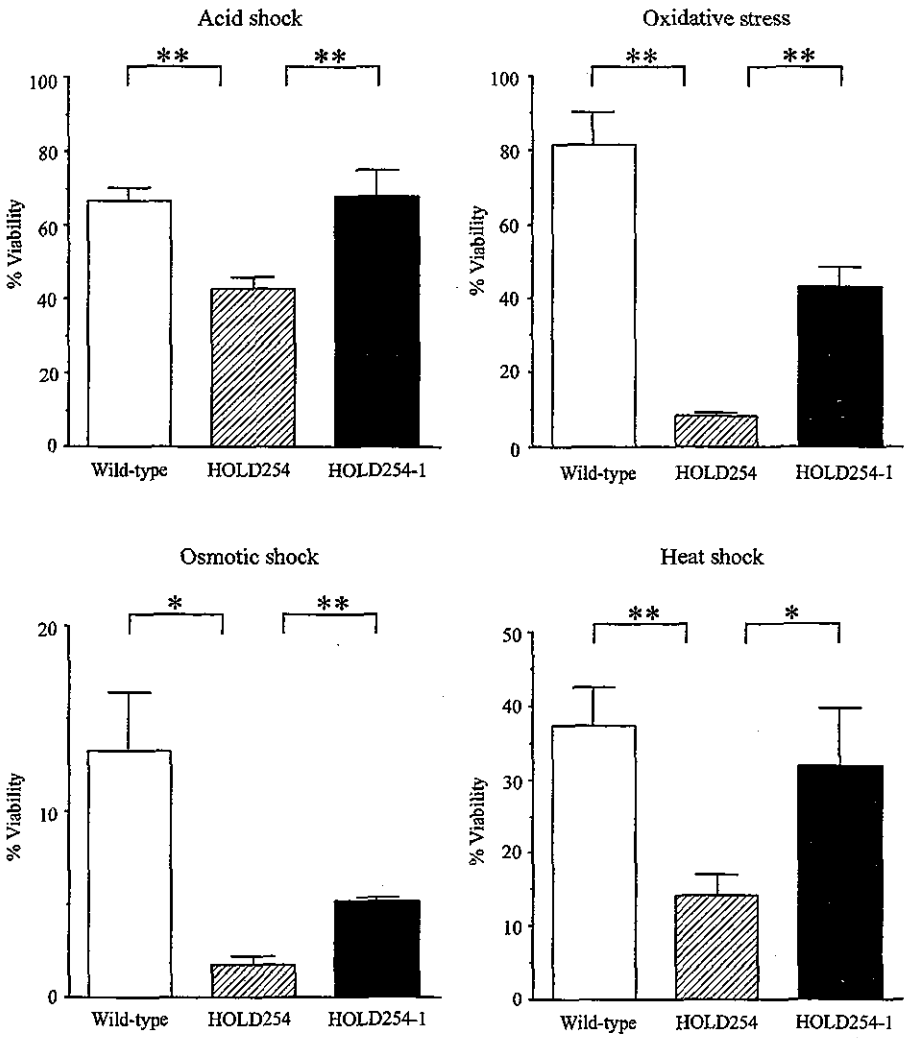

FIG. 7. Sensitivities of in vitro-grown stationary-phase wild-type *L. dumoffii* (open bars), the *djlA* mutant strain (hatched bars), and the *djlA* complemented strain (solid bars) to oxidative stress, osmotic stress, acid stress, and heat shock (10 mM hydrogen peroxide for 30 min, 5 M sodium chloride for 30 min, pH 3 for 5 min, and 48°C for 60 min, respectively). Stationary-phase cultures were exposed to each stress as described in Materials and Methods. The percentage of viable bacteria was calculated by dividing the CFU obtained from plating the bacteria onto BCYE agar plates following exposure to the indicated stress by the CFU of the bacteria obtained from plating the bacteria onto BCYE agar plates prior to exposure to the stress and multiplying by 100. Experiments were performed at least three times, and the results represent the mean and standard deviation. Results were analyzed for significance by analysis of variance and by a two-tailed, unpaired *t* test. Asterisks indicate significant differences between the *djlA* mutant and two other strains. (*, $P < 0.01$; **, $P < 0.001$).

reported that *L. pneumophila* is targeted into RER-surrounding phagosomes that do not fuse with lysosomes in mammalian cells (25, 33), while *L. micdadei* is targeted into RER-free phagosomes that are thought to fuse to lysosomes in mammalian cells (3, 36). Doyle et al. (20) reported that virulent *L. longbeachae*-containing phagosomes were surrounded by RER but avirulent *L. longbeachae*-containing phagosomes did not have RER. Our observations suggest that *L. dumoffii* might replicate in phagosomes which have not fused with lysosomes and are able to recruit host cell organelles, similar to that reported for *L. pneumophila*. The *djlA* mutant seemed to be intact (Fig. 5B), and no loss of CFU was observed during the infection (Fig. 1A and 2A). It is possible that the mutant bacteria are in either a late endosomal or a nondegradative lysosomal compartment, as described by Joshi et al. (35). The frequency of recruitment of *L. dumoffii* RER at 8 h is lower than that reported for *L. pneumophila* (32). We suspect that association with ER and avoidance of lysosomes by *L. dumoffii* is temporary, as shown for *L. pneumophila* (63).

Although the precise function of DjlA is unclear, it does not seem to play a direct role in intracellular trafficking. DjlA might contribute to folding or transportation of the proteins, such as Dot/Icm proteins, which play an important role in intracellular survival and growth. Most of the Dot/Icm proteins are located in the bacterial membranes, where they may associate to form a large transport complex, the type IV secretion apparatus (17, 43, 51, 60, 61). DjlA might cooperate with Dot/Icm proteins through their interaction in the membranes, since the N-terminal portion of DjlA is located in the cytoplastic membrane (16, 37). It has been reported that the two-

component regulatory system, PhoP-PhoQ, of *Salmonella enterica* serovar Typhimurium plays an essential role in survival within macrophages (28). It is possible that DjlA promotes *L. dumoffii* to adapt to intracellular environments and to coordinate with the two-component signal transduction systems. In vitro, DjlA-deficient mutants showed an increased susceptibility to several stresses, including oxidative stress, that might be encountered by bacteria in mammalian cells. DjlA might protect the genes or proteins, including Dot/Icm and catalase-peroxidase (7), that are important for intracellular growth, from harmful stress in a direct or indirect manner. Several lines of evidence for the important role of stress proteins in intracellular growth and virulence have been reported for intracellular pathogens; these include DnaK of *Brucella suis* (38), ClpC and ClpP of *Listeria monocytogenes* (24, 54), Lon of *B. abortus* (53), and GsrA of *Yersinia enterocolitica* (69). In *L. pneumophila*, at least 30 proteins are included during the intracellular infection of macrophages and at least 13 of these proteins, including GroEL (Hsp60), GroES, and GspA, are also induced by several stress conditions in vitro (1, 2, 21). Recently, Pedersen et al. (50) demonstrated direct evidence for the role of the stress protein of *L. pneumophila*, HtrA, during intracellular growth in mammalian cells but not in protozoan cells. Our data indicated that DjlA plays an important role during intracellular growth in both mammalian and protozoan cells. Besides Dot/Icm proteins, stress proteins or molecular chaperones might play an important role in the intracellular growth of the *Legionella* species.

In conclusion, we showed the essential role of *L. dumoffii* Dot/Icm homologues and DjlA during the intracellular infection of mammalian cells and protozoa. The precise mechanism of DjlA involvement in intracellular multiplication, including interaction with DnaK, remains to be elucidated. Further investigation of specific substrates with which DjlA interacts will lead to a better understanding of the intracellular survival mechanism in the *Legionella* species.

ACKNOWLEDGMENTS

We acknowledge H. A. Shuman for his generous gifts of plasmids pLAW330 and the pMMB207c. We thank H. Nakayama and C. C. Sze for scientific discussion. We also thank H. Fujita, K. Iida, and H. Kajiwara for technical assistance. We thank L. Saza for manuscript preparation.

This work was supported by grants-in-aid for scientific research (B)(2)14370094, (B)(1)12490009, and (C)(2)15590391 from the Ministry of Education, Science, Culture and Sports of Japan. This work was also supported by Health and Labour Sciences research grants (H15-Ganyobou-095) from the Ministry of Health, Labour and Welfare.

REFERENCES

1. **Abu Kwaik, Y., B. I. Eisenstein, and N. C. Engleberg.** 1993. Phenotypic modulation by *Legionella pneumophila* upon infection of macrophages. Infect. Immun. **61**:1320–1329.
2. **Abu Kwaik, Y., L. Y. Gao, O. S. Harb, and B. J. Stone.** 1997. Transcriptional regulation of the macrophage-induced gene (*gspA*) of *Legionella pneumophila* and phenotypic characterization of a null mutant. Mol. Microbiol. **24**:629–642.
3. **Abu Kwaik, Y., C. Venkataraman, O. S. Harb, and L. Y. Gao.** 1998. Signal transduction in the protozoan host *Hartmannella vermiformis* upon attachment and invasion by *Legionella micdadei*. Appl. Environ. Microbiol. **64**: 3134–3139.
4. **Alli, O. A., S. Zink, N. K. Von Lackum, and Y. Abu-Kwaik.** 2003. Comparative assessment of virulence traits in *Legionella* spp. Microbiology **149**:631–641.
5. **Andrews, H. L., J. P. Vogel, and R. R. Isberg.** 1998. Identification of linked *Legionella pneumophila* genes essential for intracellular growth and evasion of the endocytic pathway. Infect. Immun. **66**:950–958.
6. **Baine, W. B.** 1985. Cytolytic and phospholipase C activity in *Legionella* species. J. Gen. Microbiol. **131**:1383–1391.
7. **Bandyopadhyay, P., B. Byrne, Y. Chan, M. S. Swanson, and H. M. Steinman.** 2003. *Legionella pneumophila* catalase-peroxidases are required for proper trafficking and growth in primary macrophages. Infect. Immun. **71**:4526–4535.
8. **Benin, A. L., R. F. Benson, and R. E. Besser.** 2002. Trends in legionnaires disease, 1980–1998: declining mortality and new patterns of diagnosis. Clin. Infect. Dis. **35**:1039–1046.
9. **Bozue, J. A., and W. Johnson.** 1996. Interaction of *Legionella pneumophila* with *Acanthamoeba castellanii*: uptake by coiling phagocytosis and inhibition of phagosome-lysosome fusion. Infect. Immun. **64**:668–673.
10. **Brabetz, W., C. E. Schirmer, and H. Brade.** 2000. 3-Deoxy-D-*manno*-oct-2-ulosonic acid (Kdo) transferase of *Legionella pneumophila* transfers two Kdo residues to a structurally different lipid A precursor of *Escherichia coli*. J. Bacteriol. **182**:4654–4657.
11. **Brenner, D. J.** 1985. The new species of *Legionella*. Int. J. Syst. Bacteriol. **35**:50–59.
12. **Byrne, B., and M. S. Swanson.** 1998. Expression of *Legionella pneumophila* virulence traits in response to growth conditions. Infect. Immun. **66**:3029–3034.
13. **Casaregola, S., M. Chen, N. Bouquin, V. Norris, A. Jacq, M. Goldberg, S. Margarson, M. Tempete, S. McKenna, H. Sweetman, et al.** 1991. Analysis of a myosin-like protein and the role of calcium in the *E. coli* cell cycle. Res. Microbiol. **142**:201–207.
14. **Chen, L., Y. Chen, D. W. Wood, and E. W. Nester.** 2002. A new type IV secretion system promotes conjugal transfer in *Agrobacterium tumefaciens*. J. Bacteriol. **184**:4838–4845.
15. **Clarke, D. J., L. B. Holland, and A. Jacq.** 1997. Point mutations in the transmembrane domain of DjlA, a membrane-linked DnaJ-like protein, abolish its function in promoting colanic acid production via the Res signal transduction pathway. Mol. Microbiol. **25**:933–944.
16. **Clarke, D. J., A. Jacq, and I. B. Holland.** 1996. A novel DnaJ-like protein in *Escherichia coli* inserts into the cytoplasmic membrane with a type III topology. Mol. Microbiol. **20**:1273–1286.
17. **Coers, J., J. C. Kagan, M. Matthews, H. Nagai, D. M. Zuckman, and C. R. Roy.** 2000. Identification of Icm protein complexes that play distinct roles in the biogenesis of an organelle permissive for *Legionella pneumophila* intracellular growth. Mol. Microbiol. **38**:719–736.
18. **Cordes, L. G., H. W. Wilkinson, G. W. Gorman, B. J. Fikes, and D. W. Fraser.** 1979. Atypical *Legionella*-like organisms: fastidious water-associated bacteria pathogenic for man. Lancet **ii**:927–930.
19. **Da Silva, T. R., J. R. De Freitas, Q. C. Silva, C. P. Figueira, E. Roxo, S. C. Leao, I. A. De Freitas, and P. S. Veras.** 2002. Virulent *Mycobacterium fortuitum* restricts NO production by a gamma interferon-activated J774 cell line and phagosome-lysosome fusion. Infect. Immun. **70**:5628–5634.
20. **Doyle, R. M., N. P. Cianciotto, S. Banvi, P. A. Manning, and M. W. Heuzenroeder.** 2001. Comparison of virulence of *Legionella longbeachae* strains in guinea pigs and U937 macrophage-like cells. Infect. Immun. **69**:5335–5344.
21. **Fernandez, R. C., S. M. Logan, S. H. Lee, and P. S. Hoffman.** 1996. Elevated levels of *Legionella pneumophila* stress protein Hsp60 early in infection of human monocytes and L929 cells correlate with virulence. Infect. Immun. **64**:1968–1976.
22. **Fields, B. S.** 1996. The molecular ecology of legionellae. Trends Microbiol. **4**:286–290.
23. **Furuno, K., T. Ishikawa, K. Akasaki, S. Yano, Y. Tanaka, Y. Yamaguchi, H. Tsuji, M. Himeno, and K. Kato.** 1989. Morphological localization of a major lysosomal membrane glycoprotein in the endocytic membrane system. J. Biochem. (Tokyo) **106**:708–716.
24. **Gaillot, O., E. Pellegrini, S. Bregenholt, S. Nair, and P. Berche.** 2000. The ClpP serine protease is essential for the intracellular parasitism and virulence of *Listeria monocytogenes*. Mol. Microbiol. **35**:1286–1294.
25. **Gao, L. Y., O. S. Harb, and Y. A. Kwaik.** 1998. Identification of macrophage-specific infectivity loci (*mil*) of *Legionella pneumophila* that are not required for infectivity of protozoa. Infect. Immun. **66**:883–892.
26. **Genevaux, P., F. Schwager, C. Georgopoulos, and W. L. Kelley.** 2001. The *djlA* gene acts synergistically with *dnaJ* in promoting *Escherichia coli* growth. J. Bacteriol. **183**:5747–5750.
27. **Genevaux, P., A. Wawrzynow, M. Zylicz, C. Georgopoulos, and W. L. Kelley.** 2001. DjlA is a third DnaK co-chaperone of *Escherichia coli*, and DjlA-mediated induction of colanic acid capsule requires DjlA-DnaK interaction. J. Biol.Chem. **276**:7906–7912.
28. **Groisman, E. A.** 2001. The pleiotropic two-component regulatory system PhoP-PhoQ. J. Bacteriol. **183**:1835–1842.
29. **Hales, L. M., and H. A. Shuman.** 1999. The *Legionella pneumophila rpoS* gene is required for growth within *Acanthamoeba castellanii*. J. Bacteriol. **181**:4879–4889.
30. **Hanahan, D.** 1983. Studies on transformation of *Escherichia coli* with plasmids. J. Mol. Biol. **166**:557–580.
31. **Hohn, B., and J. Collins.** 1980. A small cosmid for efficient cloning of large DNA fragments. Gene **11**:291–298.

32. **Horwitz, M. A.** 1983. Formation of a novel phagosome by the Legionnaires' disease bacterium (*Legionella pneumophila*) in human monocytes. J. Exp. Med. **158**:1319–1331.
33. **Horwitz, M. A.** 1983. The Legionnaires' disease bacterium (*Legionella pneumophila*) inhibits phagosome-lysosome fusion in human monocytes. J. Exp. Med. **158**:2108–2126.
34. **Horwitz, M. A., and F. R. Maxfield.** 1984. *Legionella pneumophila* inhibits acidification of its phagosome in human monocytes. J. Cell Biol. **99**:1936–1943.
35. **Joshi, A. D., S. Sturgill-Koszycki, and M. S. Swanson.** 2001. Evidence that Dot-dependent and -independent factors isolate the *Legionella pneumophila* phagosome from the endocytic network in mouse macrophages. Cell. Microbiol. **3**:99–114.
36. **Joshi, A. D., and M. S. Swanson.** 1999. Comparative analysis of *Legionella pneumophila* and *Legionella micdadei* virulence traits. Infect. Immun. **67**: 4134–4142.
37. **Kelley, W. L., and C. Georgopoulos.** 1997. Positive control of the two-component RcsC/B signal transduction network by DjlA: a member of the DnaJ family of molecular chaperones in *Escherichia coli*. Mol. Microbiol. **25**:913–931.
38. **Kohler, S., J. Teyssier, A. Cloeckaert, B. Rouot, and J. P. Liautard.** 1996. Participation of the molecular chaperone DnaK in intracellular growth of *Brucella suis* within U937-derived phagocytes. Mol. Microbiol. **20**:701–712.
39. **Kuronita, T., E. L. Eskelinen, H. Fujita, P. Saftig, M. Himeno, and Y. Tanaka.** 2002. A role for the lysosomal membrane protein LGP85 in the biogenesis and maintenance of endosomal and lysosomal morphology. J. Cell Sci. **115**:4117–4131.
40. **Lewallen, K. R., R. M. McKinney, D. J. Brenner, C. W. Moss, D. H. Dail, B. M. Thomason, and R. A. Bright.** 1979. A newly identified bacterium phenotypically resembling, but genetically distinct from, *Legionella pneumophila*: an isolate in a case of pneumonia. Ann. Intern. Med. **91**:831–834.
41. **Maruta, K., H. Miyamoto, T. Hamada, M. Ogawa, H. Taniguchi, and S. Yoshida.** 1998. Entry and intracellular growth of *Legionella dumoffii* in alveolar epithelial cells. Am. J. Respir. Crit. Care Med. **157**:1967–1974.
42. **Maruta, K., M. Ogawa, H. Miyamoto, K. Izu, and S. I. Yoshida.** 1998. Entry and intracellular localization of *Legionella dumoffii* in Vero cells. Microb. Pathog. **24**:65–73.
43. **Matthews, M., and C. R. Roy.** 2000. Identification and subcellular localization of the *Legionella pneumophila* IcmX protein: a factor essential for establishment of a replicative organelle in eukaryotic host cells. Infect. Immun. **68**:3971–3982.
44. **Miyamoto, H., H. Taniguchi, and S. Yoshida.** 2003. A simple qualitative assay for intracellular growth of *Legionella pneumophila* within *Acanthamoeba culbertsoni*. Kansenshogaku Zasshi. **77**:343–345. (In Japanese)
45. **Miyamoto, H., S. I. Yoshida, H. Taniguchi, and H. A. Shuman.** 2003. Virulence conversion of *Legionella pneumophila* by conjugal transfer of chromosomal DNA. J. Bacteriol. **185**:6712–6718.
46. **Moffat, J. F., and L. S. Tompkins.** 1992. A quantitative model of intracellular growth of *Legionella pneumophila* in *Acanthamoeba castellanii*. Infect. Immun. **60**:296–301.
47. **Morales, V. M., A. Backman, and M. Bagdasarian.** 1991. A series of wide-host-range low-copy-number vectors that allow direct screening for recombinants. Gene **97**:39–47.
48. **Nagai, H., and C. R. Roy.** 2001. The DotA protein from *Legionella pneumophila* is secreted by a novel process that requires the Dot/Icm transporter. EMBO J. **20**:5962–5970.
49. **Padmalayam, I., K. Karem, B. Baumstark, and R. Massung.** 2000. The gene encoding the 17-kDa antigen of *Bartonella henselae* is located within a cluster of genes homologous to the *virB* virulence operon. DNA Cell Biol. **19**:377–382.
50. **Pedersen, L. L., M. Radulic, M. Doric, and Y. Abu Kwaik.** 2001. HtrA homologue of *Legionella pneumophila*: an indispensable element for intracellular infection of mammalian but not protozoan cells. Infect. Immun. **69**:2569–2579.
51. **Purcell, M., and H. A. Shuman.** 1998. The *Legionella pneumophila icmGCDJBF* genes are required for killing of human macrophages. Infect. Immun. **66**:2245–2255.
52. **Quinn, F. D., M. G. Keen, and L. S. Tompkins.** 1989. Genetic, immunological, and cytotoxic comparisons of *Legionella* proteolytic activities. Infect. Immun. **57**:2719–2725.
53. **Robertson, G. T., M. E. Kovach, C. A. Allen, T. A. Ficht, and R. M. Roop, Jr.** 2000. The *Brucella abortus* Lon functions as a generalized stress response protease and is required for wild-type virulence in BALB/c mice. Mol. Microbiol. **35**:577–588.
54. **Rouquette, C., C. de Chastellier, S. Nair, and P. Berche.** 1998. The ClpC ATPase of *Listeria monocytogenes* is a general stress protein required for virulence and promoting early bacterial escape from the phagosome of macrophages. Mol. Microbiol. **27**:1235–1245.
55. **Roy, C. R., K. H. Berger, and R. R. Isberg.** 1998. *Legionella pneumophila* DotA protein is required for early phagosome trafficking decisions that occur within minutes of bacterial uptake. Mol. Microbiol. **28**:663–674.
56. **Roy, C. R., and L. G. Tilney.** 2002. The road less traveled: transport of *Legionella* to the endoplasmic reticulum. J. Cell Biol. **158**:415–419.
57. **Sadosky, A. B., L. A. Wiater, and H. A. Shuman.** 1993. Identification of *Legionella pneumophila* genes required for growth within and killing of human macrophages. Infect. Immun. **61**:5361–5373.
58. **Sambrook, J., and W. J. Russell.** 2001. Molecular cloning: a laboratory manual, 3rd ed. Cold Spring Harbor Laboratory Press, Cold Spring Harbor, N.Y.
59. **Schulein, R., and C. Dehio.** 2002. The VirB/VirD4 type IV secretion system of *Bartonella* is essential for establishing intraerythrocytic infection. Mol. Microbiol. **46**:1053–1067.
60. **Segal, G., M. Purcell, and H. A. Shuman.** 1998. Host cell killing and bacterial conjugation require overlapping sets of genes within a 22-kb region of the *Legionella pneumophila* genome. Proc. Natl. Acad. Sci. USA **95**:1669–1674.
61. **Segal, G., and H. A. Shuman.** 1998. How is the intracellular fate of the *Legionella pneumophila* phagosome determined? Trends Microbiol. **6**:253–255.
62. **Small, P. L., L. Ramakrishnan, and S. Falkow.** 1994. Remodeling schemes of intracellular pathogens. Science **263**:637–639.
63. **Sturgill-Koszycki, S., and M. S. Swanson.** 2000. *Legionella pneumophila* replication vacuoles mature into acidic, endocytic organelles. J. Exp. Med. **192**:1261–1272.
64. **Ueguchi, C., M. Kakeda, H. Yamada, and T. Mizuno.** 1994. An analogue of the DnaJ molecular chaperone in *Escherichia coli*. Proc. Natl. Acad. Sci. USA **91**:1054–1058.
65. **Ueguchi, C., T. Shiozawa, M. Kakeda, H. Yamada, and T. Mizuno.** 1995. A study of the double mutation of *dnaJ* and *cbpA*, whose gene products function as molecular chaperones in *Escherichia coli*. J. Bacteriol. **177**:3894–3896.
66. **Wai, S. N., Y. Mizunoe, A. Takade, S. I. Kawabata, and S. I. Yoshida.** 1998. *Vibrio cholerae* O1 strain TSI-4 produces the exopolysaccharide materials that determine colony morphology, stress resistance, and biofilm formation. Appl. Environ. Microbiol. **64**:3648–3655.
67. **Wall, D., M. Zylicz, and C. Georgopoulos.** 1994. The NH_2-terminal 108 amino acids of the *Escherichia coli* DnaJ protein stimulate the ATPase activity of DnaK and are sufficient for lambda replication. J. Biol. Chem. **269**:5446–5451.
68. **Wiater, L. A., A. B. Sadosky, and H. A. Shuman.** 1994. Mutagenesis of *Legionella pneumophila* using Tn*903* dI*lacZ*: identification of a growth-phase-regulated pigmentation gene. Mol. Microbiol. **11**:641–653.
69. **Yamamoto, T., T. Hanawa, S. Ogata, and S. Kamiya.** 1996. Identification and characterization of the *Yersinia enterocolitica gsrA* gene, which protectively responds to intracellular stress induced by macrophage phagocytosis and to extracellular environmental stress. Infect. Immun. **64**:2980–2987.
70. **Yanisch-Perron, C., J. Vieira, and J. Messing.** 1985. Improved M13 phage cloning vectors and host strains: nucleotide sequences of the M13mp 18 and pUC19 vectors. Gene **33**:103–119.
71. **Yu, V. L., J. F. Plouffe, M. C. Pastoris, J. E. Stout, M. Schousboe, A. Widmer, J. Summersgill, T. File, C. M. Heath, D. L. Paterson, and A. Chereshsky.** 2002. Distribution of *Legionella* species and serogroups isolated by culture in patients with sporadic community-acquired legionellosis: an international collaborative survey. J. Infect. Dis. **186**:127–128.
72. **Yura, T., H. Mori, H. Nagai, T. Nagata, A. Ishihama, N. Fujita, K. Isono, K. Mizobuchi, and A. Nakata.** 1992. Systematic sequencing of the *Escherichia coli* genome: analysis of the 0–2.4 min region. Nucleic Acids Res. **20**:3305–3308.
73. **Zuber, M., T. A. Hoover, and D. L. Court.** 1995. Analysis of a *Coxiella burnetti* gene product that activates capsule synthesis in *Escherichia coli*: requirement for the heat shock chaperone DnaK and the two-component regulator RcsC. J. Bacteriol. **177**:4238–4244.
74. **Zuckman, D. M., J. B. Hung, and C. R. Roy.** 1999. Pore-forming activity is not sufficient for *Legionella pneumophila* phagosome trafficking and intracellular growth. Mol. Microbiol. **32**:990–1001.

Editor: S. H. E. Kaufmann

Confocal imaging of biofilm formation process using fluoroprobed *Escherichia coli* and fluoro-stained exopolysaccharide

Ryo Maeyama,[1,2] Yoshimitsu Mizunoe,[3] James M. Anderson,[4] Masao Tanaka,[2] Takehisa Matsuda[1]
[1]*Department of Biomedical Engineering, Faculty of Medical Sciences, Kyushu University, Maidashi, Fukuoka 812-8582, Japan*
[2]*Department of Surgery and Oncology, Faculty of Medical Sciences, Kyushu University, Maidashi, Fukuoka 812-8582, Japan*
[3]*Department of Bacteriology, Faculty of Medical Sciences, Kyushu University, Maidashi, Fukuoka 812-8582, Japan*
[4]*Department of Pathology, Case Western Reserve University, 2085, Adelbert Road, Cleveland, Ohio 44106-4907*

Received 5 March 2004; revised 17 March 2004; accepted 19 March 2004
Published online 4 June 2004 in Wiley InterScience (www.interscience.wiley.com). DOI: 10.1002/jbm.a.30077

Abstract: We developed a novel method of evaluating biofilm architecture on a synthetic material using green fluorescent protein-expressing *Escherichia coli* and red fluorescence staining of exopolysaccharides. Confocal laser scanning microscopy observation revealed the time course of the change in the *in situ* three-dimensional structural features of biofilm on a polyurethane film without structural destruction: initially adhered cells are grown to form cellular aggregates and secrete exopolysaccharides. These cells were spottily distributed on the surface at an early incubation time but fused to form a vertically grown biofilm with incubation time. Fluorescence intensity, which is a measure of the number of cells, determined using a fluorometer and biofilm thickness determined from confocal laser scanning microscopy vertical images were found to be effective for quantification of time-dependent growth of biofilms. The curli (surface-located fibers specifically binding to fibronectin and laminin)-producing *Escherichia coli* strain, YMel, significantly proliferated on fibronectin-coated polyurethane, whereas the curli-deficient isogenic mutant, YMel-1, did not. The understanding of biofilm architecture in molecular and morphological events and new fluorescence microscopic techniques may help in the logical surface design of biomaterials with a high antibacterial potential. © 2004 Wiley Periodicals, Inc. J Biomed Mater Res 70A: 274–282, 2004

Key words: biofilm; green fluorescent protein; confocal laser scanning microscopy; *Escherichia coli*; curli

INTRODUCTION

The biomass of bacteria and extracellular materials including exopolysaccharides (EPS) that accumulate on synthetic substrates is called a biofilm.[1,2] Once a biofilm is formed on artificial implants in the body, serious, often life-threatening events or situations such as "septic shock," defined as a systemic response to infection, occur, which cannot be managed by antimicrobial drug administration due to a high level of resistance to drug diffusion into the well-stabilized biofilm bioarchitecture.[3] Implanted artificial prostheses, which are often associated with biomaterial-based biofilms, include cardiovascular implants, orthopedic replacements, intraocular implants, and intravascular catheters. Biliary stents and urinary catheters are often occluded by biofilms of *Escherichia coli*, resulting in complications in patients.[4] For cardiovascular implants, a second surgery to replace a bacterial-infected implant with a new one is often necessary.

The microbial colonization, and the nature and architecture of biofilms on synthetic polymers have been studied over a few decades. Previous studies have revealed various aspects of biofilms qualitatively as well as quantitatively, particularly focusing on adhered and proliferated cells by microscopy, plate counting, or dye-staining technique.[5–8] Electron microscopy has been used to observe the three-dimen-

Correspondence to: T. Matsuda; e-mail: matsuda@med.kyushu-u.ac.jp
Contract grant sponsor: Ministry of Health, Labour and Welfare (MHLW) of Japan, Grant-in-Aid for Scientific Research
Contract grant sponsor: Ministry of Education, Culture, Sports, Science, and Technology (MEXT) of Japan, Grant-in-Aid for Scientific Research and for the Creation of Innovations through Business-Academic-Public Sector Cooperation
Contract grant sponsor: NIH/NIBIB; contract grant number: EB-00279

sional (3D) structural features of biofilms.[9] However, this method often destroys biofilms because of complicated fixation procedures such as dehydration and fails to show an "as-is" structure.[10] Therefore, the formation of an as-is 3D structure of a biofilm of *E. coli* on synthetic polymers has not yet been fully understood.

Confocal laser scanning microscopy (CLSM) enables the high-resolution fluorescence imaging and deep optical sectioning of biological structures with negligible background interface. Additionally, CLSM enables a biofilm to be observed under hydrated conditions, thus maintaining an as-is structure without structure destruction.[11] When combined with fluorescent probes, CLSM can be effectively used for the visualization of biofilm components. In recent years, green fluorescent protein (GFP) from jellyfish *Aequorea victoria* has emerged as an *in situ* marker of living cells. EPS, which are produced by *E. coli* and which serve as structural anchors for bacterial cells in biofilms, can be specifically stained with a fluorescent dye, rhodamine-labeled lectin.[12,13] The co-use of GFP-expressing *E. coli* and rhodamine-labeled lectin under CLSM enables us to obtain in-depth information on the distribution state of the bacterial and EPS components of 3D biofilms.

The objective of this study was to perform an *in situ* visualization of the 3D structure of *E. coli*–based biofilm on polyurethane (PU) films. *In situ* monitoring using the CLSM technique enabled us to analyze the time-dependent construction of 3D-structured biofilms on a synthetic polymer. Two *E. coli* strains, curli-producing (YMel) and curli-deficient (YMel-1), were used.[14,15] Curli are surface organelles of *E. coli*, which are composed of thin fibers with a diameter of approximately 2 nm that mediate binding to adhesive proteins specific to fibronectin and laminin found in the eucaryotic extracellular matrix.[16] The significant role of curli in biofilm formation on a fibronectin-precoated substrate was clearly demonstrated.

MATERIALS AND METHODS

Bacterial strains and plasmid

The *E. coli* strains used in this study were the curli-producing strain YMel and the curli-deficient isogenic mutant strain YMel-1, both of which were transformed by electroporation with the *gfp*mut3* gene encoding plasmid DNA (pJBA27) and expressing a stable green fluorescent protein (Gfpmut3*) as previously reported.[17] *E. coli* from the frozen bacterial solution was cultured in 3 mL of modified Luria-Bertani medium containing 50 μg/mL ampicillin and 3 g/L NaCl at 37°C for 18 h under aerobic conditions, and then scaled up to a concentration of approximately 2×10^8 colony forming units per milliliter (CFU/mL), which was determined by the plate count method. Then they were diluted to a concentration of 2×10^5 CFU/mL, which was used as an initial concentration for experiments.

CLSM

The biofilms were examined by CLSM (Radiance 2000; BioRad, Hercules, CA). Square PU sheets (obtained from Olympus Optical Co., Ltd., Tokyo, Japan), which were cut to fit a six-well cell culture cluster, were sterilized using ethylene oxide, placed in a six-well cell culture cluster using sterilized forceps, and incubated with *E. coli* cell suspension (2×10^5 CFU/mL) under static condition. After 3-, 6-, 12-, and 24-h incubations, culture medium was removed and phosphate-buffered saline (PBS) was gently added to prevent drying of the biofilms. To visualize the EPS of the biofilms, rhodamine-labeled concanavalin A (5 μg/mL; Vector Laboratories, Burlingame, CA), which specifically binds to D-(+)-glucose and D-(+)-mannose groups on EPS, was used. One hundred microliters of this fluorescent solution was carefully applied on top of the biofilms grown on the PU sheet. After a 30-min incubation in the dark at room temperature, the excess staining solution was removed by four rinses with PBS. Images were recorded at an excitation wavelength of 488 nm and an emission wavelength of 515 ± 30 nm for GFP and at an excitation wavelength of 514 nm and an emission wavelength of 600 ± 50 nm for rhodamine-labeled concanavalin A.

Electron microscopy

For negative staining, *E. coli* cells, harvested from the biofilm formed on the PU sheet after a 24-h incubation, were mixed with distilled water, and the suspension was allowed to sediment for 2 min on a grid. After washing with distilled water, the specimen was negatively stained with 2% uranyl formiate and air dried before transmission electron microscopy (H-7000E; Hitachi, Tokyo, Japan).

For scanning electron microscopy (SEM), the biofilm grown on a glass slide (Matsunami Glass Industries Ltd., Osaka, Japan) after a 24-hr incubation was fixed in 2% glutaraldehyde (Electron Microscopy Sciences, Hatfield, PA) in 0.1*M* phosphate buffer for 1 h at room temperature. The fixed samples were dehydrated for 20 min at each step in an ascending acetone series, sputter-coated with platinum, and evaluated by SEM (JSM-840A; JEOL, Tokyo, Japan).

Bacterial adhesion study

The adhesion of bacteria was studied under static condition. Round PU sample sheets sterilized by ethylene oxide were placed in a 24-well cell culture cluster using sterilized forceps and incubated with *E. coli*. After 3-, 6-, 12-, and 24-h incubations, the round PU sheets were rinsed with PBS,

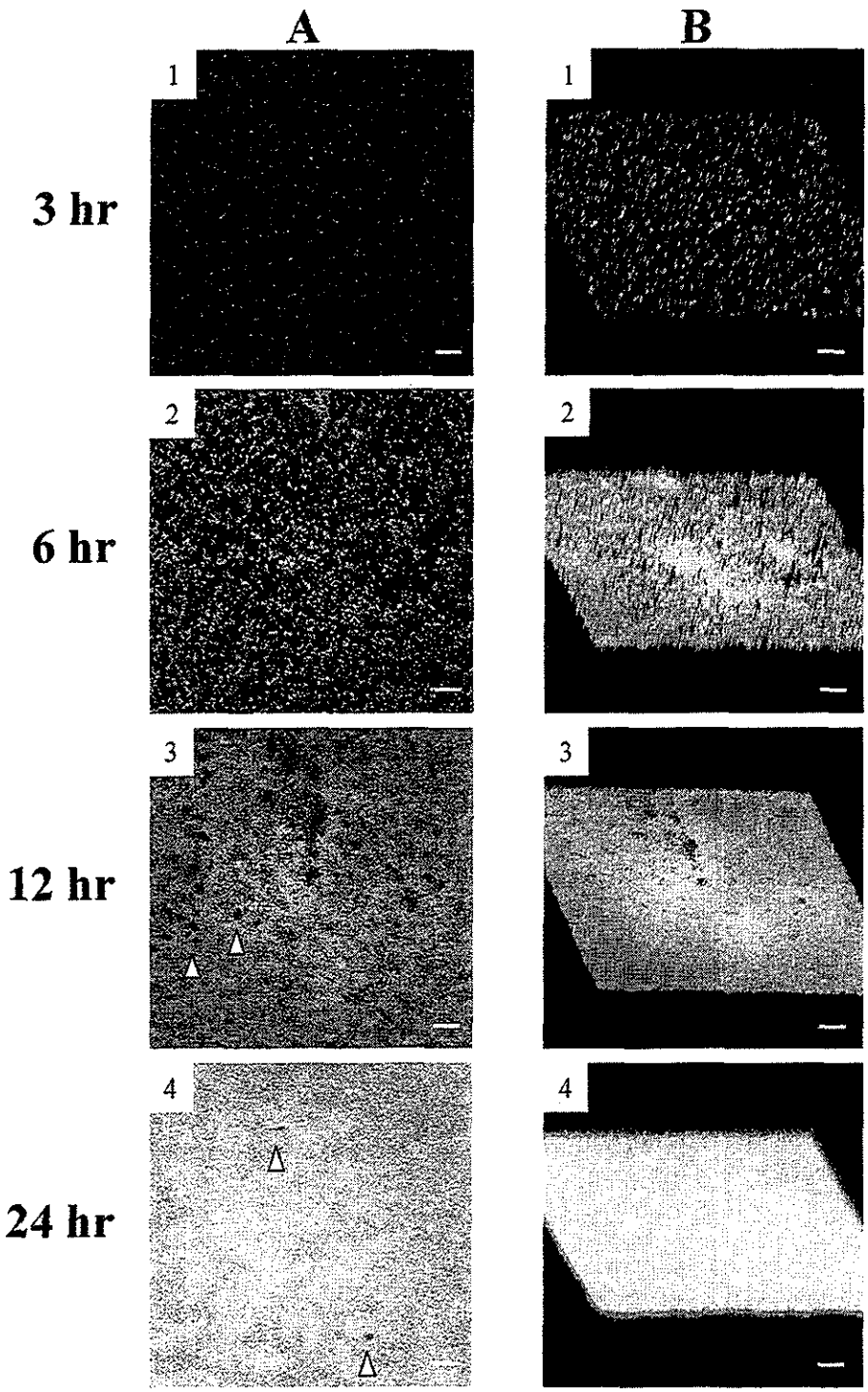

Figure 1. CLSM photographs of biofilms on PU at 3, 6, 12, and 24 h of incubations. (A) top view; (B) oblique view. Bar: 100 μm. Green and red areas indicate *E. coli* (expressing GFP) and EPS (stained with rhodamine-labeled concanavalin A), respectively. Irregular dark spots indicate water channels (white arrowheads).

placed in 15-mL Eppendorf tubes with 2 mL of PBS and sonicated for 60 s. Complete detachment of bacterial cells from the round sheets after 60-s sonication was confirmed by CLSM. Then, 100 μL of the solution containing detached bacterial cells was placed in a 96-well cell culture cluster and fluorescence intensity was measured with Molecular Imager FX (BioRad). Viable bacterial cells (CFU/cm^2) were also counted by the plate count method. Experiments were run with five samples, and the mean and standard deviation were recorded.

biofilm formation was stained with rhodamine-labeled concanavalin A. The biofilm was observed using CLSM with time. Figure 1 shows (A) top-view and (B) oblique-view images of biofilms. At 3 h of incubation, adhered YMel cells (green color) randomly distributed without aggregate formation, and the EPS (red) formed regionally exhibited a thin cloudlike structure. At 6 h of incubation, the number of adhered YMel cells increased to form heterogeneous mosaic colonies composed of small aggregates that are scattered all over the substrate, and high-intensity red EPS regions tended to enlarge to cover the majority of the surface, thus initiating the formation of 3D structural constructs. The coexisting regions composed of green cells and red EPS were observed as a yellow region [Fig. 1(2B)]. At 12 h of incubation, the surface was completely covered with green (a major continuous matrix phase), yellow, and some spotty red regions (a dispersed domain). A small number of irregular dark spots were observed, which are supposed to be water channels, as described in the Discussion section. At 24 h of incubation, almost the entire surface area was yellowish-green, and the oblique-view CLSM image suggests that a thick biofilm was formed.

Figure 2(A) shows the time-lapse images of the vertical sections of biofilms. At the initial phase, spotty aggregates and single cells, which scattered horizontally but elongated vertically, were observed. At 6 h of incubation, the number of aggregates increased horizontally and formed a filmlike structure which enabled thickness measurement. At 12 h of incubation, the biofilm appeared more tightly packed. At 24 h of incubation, the vertical cross-sectional image revealed that EPS (yellow area) are predominantly located in the midlayer of the biofilm. To examine change in thickness with time, 10 vertical lines were randomly chosen for the measurement on each image for 6-, 12-, and 24-h incubations. Figure 2(B) shows that the average thickness of biofilms gradually increased with incubation time within the experimentally observed period.

Electron microscopic observation

The biofilm grown on glass for 24 h was observed using SEM. Figure 3 shows that *E. coli* and EPS, the matrix of the biofilm, formed a complex 3D structure. Irregularly shaped spaces resembling water channels were observed among dense structures. To confirm the expression of curli, which specifically bind to fibronectin and laminin, on the surface of *E. coli* YMel in the biofilm, negative staining was performed. Figure 4 shows a fine structure composed of thin fibers that suggest curli expression in YMel, but such a structure was not found in the curli-deficient mutant YMel-1.

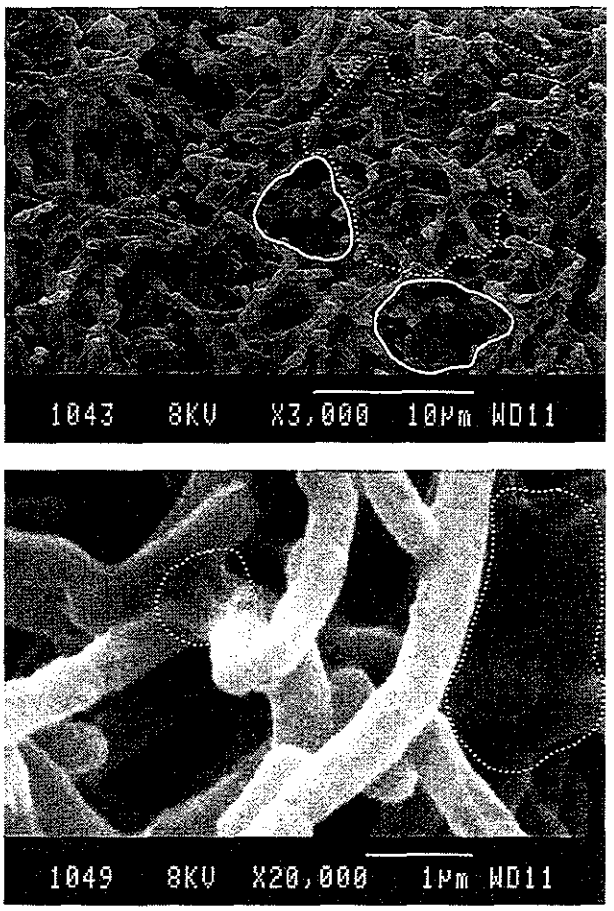

Figure 3. SEM photographs of biofilm on a glass slide at 24 h of incubation. Solid and broken lines indicate water channel regions and the dense parts of the biofilm, respectively.

Quantitative analysis

To quantify YMel cells that adhered to the PU film, round PU sheets that were incubated with YMel cells for up to 24 h postplating under static condition were subjected to gentle washing with PBS to remove nonadhering YMel cells, and then sonicated in PBS to detach all the adhered YMel cells. The fluorescence intensity of PBS containing detached YMel cells was measured with a fluorometer. In principle, the fluorescence intensity derived from GFP should correlate with the number of detached viable YMel cells by the plate count method. In fact, as shown in Figure 5, the fluorescence intensity highly correlated with the number of viable cells (correlation factor: 0.9997). The effect of the initial concentrations of YMel cells (2×10^3, 2×10^4, and 2×10^5 CFU/mL) on proliferation was studied (Fig. 6). The fluorescence intensity of PBS containing detached YMel cells increased as the initial cell concentration increased for up to 12 h of incubation. The higher the initial cell concentration, the higher the growth rate. However, after 12-h incubation, the flu-